A ROBUST METHOD TO DISCOVER CAUSAL OR ANTICAUSAL RELATION

Anonymous authors
Paper under double-blind review

ABSTRACT

Understanding whether the data generative process follows causal or anticausal relations is important for many applications. Existing causal discovery methods struggle with high-dimensional perceptual data such as images. Moreover, they require well-labeled data, which may not be feasible due to measurement error. In this paper, we propose a robust method to detect whether the data generative process is causal or anticausal. To determine the causal or anticausal relation, we identify an asymmetric property: under the causal relation, the instance distribution does not contain information about the noisy class-posterior distribution. We also propose a practical method to verify this via a noise injection approach. Our method is robust to label errors and is designed to handle both large-scale and high-dimensional datasets effectively. Both theoretical analyses and empirical results on a variety of datasets demonstrate the effectiveness of our proposed method in determining the causal or anticausal direction of the data generative process.

1 INTRODUCTION

In a dataset containing feature variables and a class variable, the dataset is considered to have a *causal* relation if some feature variables cause the class variable, but the class variable does not cause the feature variables. Conversely, the dataset is considered to have a *anticausal* relation if the class variable causes some feature variables.

Understanding whether a dataset follows causal or anticausal relations is crucial for strategic decision-making across different domains. In semi-supervised learning (SSL), correctly identifying causal and anticausal relations helps determine whether SSL methods should be used to improve predictions (Kügelgen et al., 2020). In transfer learning, understanding these relations reveals distribution shifts and guides the selection of appropriate transfer strategies (Schölkopf et al., 2012). Additionally, there are many other potential applications in causal discovery (Peters et al., 2017b; Zanga et al., 2022). For instance, in healthcare, one may want to determine whether lifestyle factors (such as exercise duration or dietary habits, which are continuous variables) lead to specific health outcomes (like the development of diabetes or heart disease, which are discrete variables). In environmental science, researchers might be interested in whether environmental conditions (such as the pollution index, which is a continuous variable) cause specific ecological events (like the occurrence of acid rain, which is a discrete variable), or if the relation is reversed.

However, in real-world applications, it is often unclear whether a dataset is causal or anticausal. Existing causal discovery methods face several challenges (*For detailed related work, please refer to Appendix. A*). The first challenge arises when dealing with datasets consisting of perceptual data, such as images or audio. In these situations, feature variables such as orientation and lighting conditions, which are hidden behind the images, are unobservable (Schölkopf et al., 2021). Most existing causal discovery methods are designed to detect relations between observed feature variables (Kalainathan et al., 2020; Shimizu et al., 2011; Huang et al., 2018; Geiger & Heckerman, 1994; Zhang & Hyvarinen, 2009; Peters et al., 2011; 2014; Chen & Chan, 2013), making them ill-suited for these types of datasets. Currently, we are unaware of any method that can effectively determine causal or anticausal relations in such datasets.

Additionally, in real-world scenarios, observed labels in large-scale datasets often contain errors (Deng et al., 2009; Xiao et al., 2015b; Li et al., 2019), which have not been considered by existing causal discovery methods. In the mining process of large-scale datasets, inexpensive but imperfect annotation methods are widely employed, such as querying commercial search engines (Li et al., 2017), downloading social media images with tags (Mahajan et al., 2018), or leveraging machine-generated labels (Kuznetsova et al., 2020). These methods inevitably yield examples with label errors. When label errors are present, the randomness of these errors affects the strength of the causal dependence between features and the observed (noisy) label $\tilde{Y}$, making it more challenging to accurately discern the true relations. Existing methods often use conditional independence tests (Zhang & Hyvarinen, 2009; Peters et al., 2011; 2014) or score optimizations (Imoto et al., 2002; Hyvärinen & Smith, 2013; Huang et al., 2018) to evaluate the strength and structure of these relations. Label errors introduce random fluctuations that distort the underlying relations between features and labels. Consequently, these tests or score optimizations may be misled by the noise, leading to inaccurate estimations of the relations.

In this paper, we introduce a robust method aimed at determining whether a dataset is causal or anticausal. We found that even when data contains label errors, it is possible to leverage observed labels $\tilde{Y}$ as they contain information about clean classes. Specifically, let $\boldsymbol{X}$ and $\tilde{Y}$ denote the instance (e.g., an image) and the observed label, respectively, there is an asymmetric property: *under anticausal datasets, the distribution of instances $P(\mathbf{X})$ can help predict observed labels $\tilde{Y}$, but this does not hold under causal datasets*. We designed a practical estimator to check this property.

Intuitively, to check whether the distribution of the instance $P(\boldsymbol{X})$ can help predict the observed label $\tilde{Y}$. We generate pseudo labels using unsupervised methods (Van Gansbeke et al., 2020; Ghosh & Lan, 2021)[1]. *In a causal dataset*, the distribution $P(\boldsymbol{X})$ does not contain useful information for predicting the observed label $\tilde{Y}$. Therefore, injecting different levels of label noise into the observed labels does not affect the (average) disagreement between pseudo labels and the observed labels. Conversely, *in an anticausal dataset*, the distribution $P(\boldsymbol{X})$ contains useful information for predicting the observed label $\tilde{Y}$. Injecting noise in this case introduces randomness, making the observed labels less predictable as the noise level increases, and thus changing the disagreement between pseudo labels and observed labels.

In Section 3.3, we theoretically prove that in a causal dataset, the disagreement between pseudo labels and observed labels remains unchanged with varying noise levels. In contrast, in an anticausal setting, the disagreement changes as the noise levels change. It is also worth noting that our RoCA estimator is general and can handle different types of label errors defined in existing literature, including random classification label errors (Wang et al., 2019), asymmetric label errors (Scott et al., 2013), manifold label errors (Cheng et al., 2022), and part-dependent label errors (Xia et al., 2020). Experimental results on 22 datasets demonstrate that our method can accurately determine whether the dataset is a causal or anticausal dataset.

2 Preliminaries

Let D be the distribution of a pair of random variables $(\boldsymbol{X}, \tilde{Y}) \in \mathcal{X} \times \{1, \ldots, C\}$, where C denotes the number of classes, $\boldsymbol{X}$ represents an instance, and $\tilde{Y}$ denotes observed label which may not be identical to the clean class Y. Given a training sample $\boldsymbol{S} = \{\boldsymbol{x}_i, \tilde{y}_i\}_{i=1}^{m}$, we aim to reveal whether the dataset is a causal or an anticausal dataset.

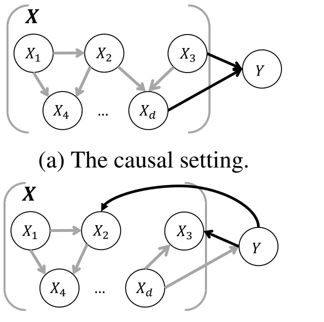

(a) The causal setting.

(b) The anticausal setting.

Figure 1: The black edge's direction determines whether a dataset is causal or anticausal dataset.

The Principle of Independent Mechanisms According to independent mechanisms (Peters et al., 2017b), the causal generative process of a system's variables consists of autonomous modules. Crucially, these modules do not inform or influence each other. In the probabilistic cases detailed in Chapter 2 of Peters et al. (2017b), the principle states that "*the conditional distribution of each variable given its causes (i.e., its mechanism) does not inform or influence the other conditional distributions.*" In other words, assuming all underlying causal variables are given and

[1] Specifically, clusters are formed based on the distribution of instances $P(\boldsymbol{X})$, and a pseudo label Y' is assigned to each cluster based on the majority of observed labels within that cluster

there are no latent variables, the conditional distributions of each variable, given all its causal parents (which can be an empty set), do not share information and are independent of each other.

Causal or Anticausal We follow the definition of Causal and Anticausal datasets from Schölkopf et al. (2012). For causal datasets, some variables in $\boldsymbol{X}$ act as causes for the class Y, and no variable in $\boldsymbol{X}$ is an effect of the class Y or shares a common cause with the class Y (e.g., Fig. 1a). In this case, Y can only be an effect of some variables in $\boldsymbol{X}$. Two distributions $P(\boldsymbol{X})$ and $P(Y|\boldsymbol{X})$ satisfy the independent causal mechanisms. The distribution $P(\boldsymbol{X})$ does not contain information about $P(Y|\boldsymbol{X})$. For anticausal datasets, the class Y causes some variables in $\boldsymbol{X}$ (e.g., Fig. 1b). In this case, the independent causal mechanisms are not satisfied for $P(\boldsymbol{X})$ and $P(Y|\boldsymbol{X})$, implying that $P(\boldsymbol{X})$ contains information about $P(Y|\boldsymbol{X})$, or $P(\boldsymbol{X})$ can help predict class Y, intuitively.

3 A Robust Causal and Anticausal Estimator

In this section, we present a practical and **Ro**bust **C**ausal and **A**nticausal (RoCA) Estimator designed to infer whether a dataset is causal or anticausal while taking into account the presence of label errors in observed labels. Note that the Assumption of our method discussed in Appendix

3.1 Rationale behind RoCA

Data Generative Processes with Label Errors *A dataset with label errors can be viewed as a result of a random process where labels are flipped based on certain probabilities*. Data generation involves two stages (see Fig. 2). Initially, an annotator is trained using a clean set Z, acquiring specific prior knowledge, θ, for the labeling task. This knowledge helps the annotator form an annotation mechanism $P_\theta(\tilde{Y}|\boldsymbol{X})$, approximating the true class posterior $P(Y|\boldsymbol{X})$. This mechanism, being correlated with $P(Y|\boldsymbol{X})$, provides insights into the true class posterior. In the annotation phase, the annotator encounters a new instance $\boldsymbol{X}$ without an observed clean class Y. Using the prior knowledge θ, the annotator assigns an observed label $\tilde{Y}$ based on $P_\theta(\tilde{Y}|\boldsymbol{X})$. This process can sometimes lead to mislabeling. It's noteworthy that $P_\theta(\tilde{Y}|\boldsymbol{X})$ *generally maintain a dependence with* $P_\theta(Y|\boldsymbol{X})$. Imagine if this dependence did not exist; the annotation mechanism $P_\theta(\tilde{Y}|\boldsymbol{X})$ would essentially be a random guess of $P(Y|\boldsymbol{X})$, rendering the observed label $\tilde{Y}$ meaningless. We will demonstrate that, due to this dependence, $P_\theta(\tilde{Y}|\boldsymbol{X})$ can serve as a surrogate for $P(Y|\boldsymbol{X})$ to help determine whether a dataset is causal or anticausal.

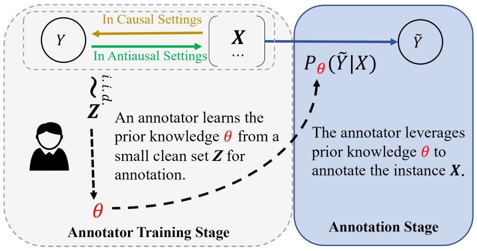
In Causal Settings
In Antiausal Settings
Y
$\boldsymbol{X}$
...
$\tilde{Y}$
$P_\theta(\tilde{Y}|X)$
i.i.d.
$\boldsymbol{Z}$
θ
An annotator learns the prior knowledge θ from a small clean set $\boldsymbol{Z}$ for annotation.
The annotator leverages prior knowledge θ to annotate the instance $\boldsymbol{X}$.
Annotator Training Stage
Annotation Stage

Figure 2: Labeling errors in annotations.

Overview In line with the principle of independent mechanisms (Peters et al., 2017b), to determine causal and anticausal relationships, one can check whether $P(\boldsymbol{X})$ can help predict $P(Y|\boldsymbol{X})$ or not. If it does, the relationship is anticausal; otherwise, it is causal. However, in the presence of label errors, the clean class Y becomes latent. Instead, we have observed labels $\tilde{Y}$ containing errors. In this case, instead of checking whether $P(\boldsymbol{X})$ contains information about $P(Y|\boldsymbol{X})$, our method checks if $P(\boldsymbol{X})$ contains information about $P_\theta(\tilde{Y}|\boldsymbol{X})$. Since $P(\tilde{Y}|X)$ can be regarded as an estimation of $P(Y|\boldsymbol{X})$ with errors. If $P(\boldsymbol{X})$ can help predict the posterior of observed labels $P(\tilde{Y}|\boldsymbol{X})$, it can also help in predicting the posterior of classes $P(Y|\boldsymbol{X})$.

$P_\theta(\tilde{Y}|\boldsymbol{X})$ Serves as a Surrogate of $P(Y|\boldsymbol{X})$ Reminding that for causal datasets, to determine whether a dataset is causal or anticausal, one can examine whether $P(\boldsymbol{X})$ can inform $P(Y|\boldsymbol{X})$. Specifically, according to the independent mechanisms (Kügelgen et al., 2020; Peters et al., 2017b), on causal datasets, $P(\boldsymbol{X})$ does not provide any information about $P(Y|\boldsymbol{X})$; on anticausal datasets, $P(\boldsymbol{X})$ generally contains information about $P(Y|\boldsymbol{X})$. However, when data contains label errors, the clean label Y is latent, estimating $P(Y|\boldsymbol{X})$ challenging. *One natural thought is to find a surrogate distribution that can help in determining the causal direction.* Specifically, the surrogate distribution should satisfy an asymmetric property with two key conditions. ***1). In a causal setting,*** $P(\boldsymbol{X})$ ***should***

not contain information about the surrogate distribution; 2). In an anticausal setting, $P(\boldsymbol{X})$ ***should contain information about the surrogate distribution.***

If such a surrogate can be found, we can infer whether a dataset is causal or anticausal by examining whether $P(\boldsymbol{X})$ contains information about the surrogate distribution. We find that $P_\theta(\tilde{Y}|\boldsymbol{X})$ fits these requirements. As it is an approximation to the underlying distribution $P(Y|\boldsymbol{X})$. It statically depends on and contains information about $P(Y|\boldsymbol{X})$. Moreover, under a causal setting, $P(\boldsymbol{X})$ cannot inform $P_\theta(\tilde{Y}|\boldsymbol{X})$, since $\tilde{Y}$ and Y are effects of $\boldsymbol{X}$, and $P(\boldsymbol{X})$ and $P_\theta(\tilde{Y}|\boldsymbol{X})$ follows causal factorization and are independent according to independent mechanisms (Peters et al., 2017b). Thus, $P_\theta(\tilde{Y}|\boldsymbol{X})$ is an proper surrogate.

Validating Whether $P(\boldsymbol{X})$ Contains Information About $P_\theta(\tilde{Y}|\boldsymbol{X})$ Building on the analysis that $P_\theta(\tilde{Y}|\mathbf{X})$ can serve as a surrogate for $P(Y|\mathbf{X})$, the remaining challenge is to effectively infer whether $P(\mathbf{X})$ contains information about $P_\theta(\tilde{Y}|\mathbf{X})$. In other words, we need to determine *whether some information learned from $P(\mathbf{X})$ can be leveraged to help predict $P_\theta(\tilde{Y}|\mathbf{X})$.* Intuitively, to achieve this, our proposed estimator employs unsupervised or self-supervised algorithms on $P(\boldsymbol{X})$ to generate clusters. We then assign a pseudo label Y' to each cluster based on the majority of observed labels within it. If these pseudo labels are informative to observed labels, it indicates that $P(\boldsymbol{X})$ contains information about $P_\theta(\tilde{Y}|\boldsymbol{X})$.

To identify regions that can help predict observed (noisy) labels, different levels of noise are manually injected into observed labels. To check if these pseudo labels are informative to observed labels, we need to validate whether each pseudo label Y' is a random guess of its corresponding observed label $\tilde{Y}$ given an instance $\boldsymbol{X}$. Specifically, let C be the number of classes, ***the asymmetric property becomes: 1). In a causal setting,*** $P(\tilde{Y}=\tilde{y}|Y'=y',\boldsymbol{X}=\boldsymbol{x})=1/C$ ***for each instance; 2). In an anticausal setting,*** $P(\tilde{Y}=\tilde{y}|Y'=y',\boldsymbol{X}=\boldsymbol{x})\neq 1/C$ ***for some instances.***

However, accurately estimating the distribution $P(\tilde{Y}|Y',\boldsymbol{X})$ from data can be challenging. Firstly, the feature vector or instance $\boldsymbol{X}$ can be high-dimensional, making the estimation of the distribution difficult due to the curse of dimensionality (Köppen, 2000). As the dimensionality increases, the data becomes sparse, requiring an exponentially larger amount of data to maintain estimation accuracy. Moreover, it is difficult to have prior knowledge or make parametric assumptions about the distribution $P(\tilde{Y}|Y',\boldsymbol{X})$, which reduces the difficulty of estimation.

Avoiding Estimation of $P(\tilde{Y}|Y',\boldsymbol{X})$ via Noise Injection To void directly estimating $P(\tilde{Y}|Y',\boldsymbol{X})$, we propose a simple and effective noise-injection method. We found that we can inject different levels of instance-dependent noise to the observed label $\tilde{Y}$, then compare the trend of the average disagreement between pseudo labels and modified labels under different levels of noise. The rationale is that, under the causal setting, $P(\boldsymbol{X})$ does not contain information about the surrogate distribution $P_\theta(\tilde{Y}|\boldsymbol{X})$. Therefore, exploiting $P(\boldsymbol{X})$ can not help predict observed labels. As a result, the pseudo labels obtained from $P(\boldsymbol{X})$ are random guesses of the observed labels. If we introduce noise to these observed labels by randomly flipping some of them, the pseudo labels should continue to guess the modified labels randomly. Since pseudo labels randomly guess any label with a fixed probability of $1/C$, the average disagreement between pseudo labels and the modified labels remains consistent, regardless of the noise level.

By contrast, in the anticausal setting, $P(\mathbf{X})$ contains information about the surrogate distribution $P_\theta(\tilde{Y}|\mathbf{X})$. This implies that pseudo labels, when derived by sufficiently exploiting $P(\mathbf{X})$, are not random guesses of the observed labels in general. As we progressively modify the observed labels by injecting increasing levels of noise, these modified labels become more random and unpredictable. This shift results in a change in the level of disagreement between the pseudo labels and the modified labels. In the end, our RoCA estimator validates the asymmetric property by examining ***whether there is a change in the average disagreement between pseudo labels (obtained through unsupervised methods) and modified labels (derived by injecting observed labels with increasing levels of noise)***.

A Toy Example To provide more intuition about the noise injection, let's consider two toy binary classification datasets illustrated in Fig. 3, where the instance $\boldsymbol{X}\in\mathbb{R}^2$. Assume that an unsupervised method separates instances into two clusters, with half of them assigned the pseudo label $Y'=0$, and the other half assigned $Y'=1$. We'll focus on instances with the pseudo label $Y'=1$, which are located in two regions (R_1 and R_2) based on their $\boldsymbol{X}$ values.

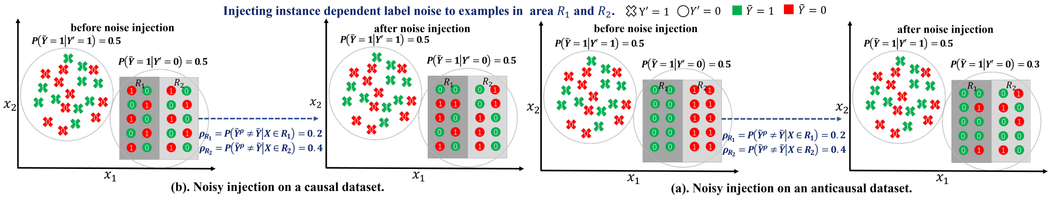
Injecting instance dependent label noise to examples in area R_1 and R_2.
$Y' = 1$
$Y' = 0$
$\tilde{Y} = 1$
$\tilde{Y} = 0$
before noise injection
$P(\tilde{Y} = 1|Y' = 1) = 0.5$
$P(\tilde{Y} = 1|Y' = 0) = 0.5$
R_1
R_2
$\rho_{R_1} = P(\tilde{Y}^\rho \neq \tilde{Y}|X \in R_1) = 0.2$
$\rho_{R_2} = P(\tilde{Y}^\rho \neq \tilde{Y}|X \in R_2) = 0.4$
after noise injection
$P(\tilde{Y} = 1|Y' = 1) = 0.5$
$P(\tilde{Y} = 1|Y' = 0) = 0.5$
x_1
x_2
(b). Noisy injection on a causal dataset.
before noise injection
$P(\tilde{Y} = 1|Y' = 1) = 0.5$
$P(\tilde{Y} = 1|Y' = 0) = 0.5$
$\rho_{R_1} = P(\tilde{Y}^\rho \neq \tilde{Y}|X \in R_1) = 0.2$
$\rho_{R_2} = P(\tilde{Y}^\rho \neq \tilde{Y}|X \in R_2) = 0.4$
after noise injection
$P(\tilde{Y} = 1|Y' = 1) = 0.5$
$P(\tilde{Y} = 1|Y' = 0) = 0.3$
(a). Noisy injection on an anticausal dataset.

Figure 3: A toy example of the change of the label disagreement via our noise injection.

In Fig. 3 (a), on a causal dataset, before noise injection, the distribution of observed labels in regions R_1 and R_2 indicate that $P(\tilde{Y} = 1|Y' = 0, \boldsymbol{X} = x) = P(\tilde{Y} = 0|Y' = 0, \boldsymbol{X} = x) = 1/2$. This suggests that each instance's pseudo label is a random guess of its observed label, rendering an average disagreement $P(\tilde{Y}^\rho = 1|Y' = 0)$ as $1/2$. after noise injection, say with an instance-dependent noise flipping 40% and 20% observed labels in regions R_1 and R_2, the average disagreement remains the same. It indicates no trend in average disagreements between pseudo labels and modified labels across different noise levels.

Fig. 3 (b) demonstrates an anticausal dataset scenario. *Despite the average disagreement for the observed label $\tilde{Y} = 0$ being 0.5, each instance's pseudo label isn't a random guess of its observed label.* Since in region R_1, all instances have the observed label $\tilde{Y} = 0$, it implies that R_1 in $P(\boldsymbol{X})$ contains information about predicting the observed label $\tilde{Y} = 0$. Similarly R_2 in $P(\boldsymbol{X})$ contains information about predicting the observed label $\tilde{Y} = 1$. This results in $P(\tilde{Y} = 1|Y' = 0, \boldsymbol{X} = x) = 1$ in region R_1 and $P(\tilde{Y} = 0|Y' = 0, \boldsymbol{X} = x) = 1$ in region R_2, deviating from the expected $1/2$. After injecting the same instance-dependent noise into observed labels in regions R_1 and R_2, the average disagreement $P(\tilde{Y}^\rho = 1|Y' = 0)$ drops to 0.3, reflecting the regions where $P(\tilde{Y} = \tilde{y}|Y' = y', \boldsymbol{X} = x)$ doesn't equal $1/C$. Thus, a trend in the average disagreements can be found under different noise levels.

3.2 Implementation of RoCA Estimator

The core idea of our method is to check if the distribution of instances $P(\boldsymbol{X})$ carries relevant information about the prediction task $P(\tilde{Y}|\boldsymbol{X})$ to determine whether a dataset is causal or anticausal. To achieve it, we generate clusters by employing advanced unsupervised methods (Van Gansbeke et al., 2020; Ghosh & Lan, 2021). Then a pseudo label Y' is assigned to each cluster based on the majority of observed labels within the cluster. To identify regions that can help predict observed (noisy) labels, different levels of noise are manually injected into observed labels. By using 0-1 loss, we calculate the average disagreements between pseudo labels and the modified labels with different injected noise levels, respectively. In a causal setting, the average disagreements remain the same under different noise levels; in an anticausal setting, the disagreement and the noise level are dependent, and a trend can be found.

Learning Pseudo Labels To learn pseudo labels, firstly, instances are clustered using a chosen unsupervised algorithm. Then each cluster is then assigned a pseudo label Y' based on the majority of observed labels within that cluster. Since our objective is to check if pseudo labels are random guesses of observed labels. Therefore the cluster number is set to be identical to the number of observed labels. More specifically, consider $K = i$ as the i-th cluster ID, and $\boldsymbol{X}_{K=i}$ as the set of instances with the i-th cluster ID, i.e.,

$$\boldsymbol{X}_{K=i} = \{\boldsymbol{x}|(\boldsymbol{x}, \tilde{y}) \in S, f(\boldsymbol{x}) = i\},$$

where f is a clustering algorithm that assigns an instance $\boldsymbol{x}$ with a cluster ID. Similarly, let $\boldsymbol{X}_{\tilde{Y}=j}$ denote the set of instances with the observed label $\tilde{Y} = j$. Let $\mathbb{1}_A$ be an indicator function that returns 1 if the event A holds true and 0 otherwise. The pseudo label Y' assigned to the instances in the set $\boldsymbol{X}_{k=i}$ is determined by applying Hungarian assignment algorithm (Jonker & Volgenant, 1986) which ensures an optimal assignment of pseudo labels to clusters such that the total number of mislabeled instances within each cluster is minimized.

An Instance-Dependent Noise Injection Our method is based on noise injection. Firstly, *the injected label noise should depend on the instance*. For example, as illustrated in Fig. 3, the noise rates of instances in different regions R_1 and R_2 are different. When noise rates for different instances are different, the disagreement between pseudo labels and modified labels changes after the noise injection on the anticausal dataset. Moreover, according to Theorem 1, in causal settings, to make disagreement between pseudo labels and modified labels remain consistent across different noise levels, the noise must be designed in a particular way. Specifically, *the design of the label-noise distribution has to fulfill that the probability of flipping an observed label to any other class is uniformly distributed*, i.e.,

$$P(\tilde{Y}^\rho = i | \tilde{Y} = j, x) = \frac{\rho_x}{C-1} \text{ for all } i \neq j, \tag{1}$$

where $\rho_x = P(\tilde{Y}^\rho \neq \tilde{Y} | X = x)$ represents the flip rate of an instance $\boldsymbol{x}$. Furthermore, $\rho = \mathbb{E}_{\boldsymbol{X}}[\rho_x]$ represents the expected noise level injected into the dataset. The notation $\tilde{Y}^\rho$ refers to the modified label after injecting a ρ-level label noise.

We implement a type of label noise that meets the aforementioned conditions. To let the designed label noise be instance dependent, we determine the flip rate magnitude based on the ℓ_1 norm of the instance $\boldsymbol{X}$. Subsequently, we set the flip rate to be uniformly distributed across other classes to fulfill Eq. (1). Specifically, for each instance in the dataset, we compute its ℓ_1 norm[2]. These computed norms are stored in a vector $\boldsymbol{A}$. Subsequently, we generate a vector $\boldsymbol{P}$ of length m, where each element represents a flip rate sampled from a truncated normal distribution ψ. The mean of the truncated normal distribution is the expected noise level to be injected, the variance is set to 1, the lower limit is 0, and the upper limit is 1. To make the label noise depend on instances, we build dependence between the instances and the sampled flip rates in $\boldsymbol{P}$ by sorting both $\boldsymbol{A}$ and $\boldsymbol{P}$ in ascending order. As a result, the instance with a smaller ℓ_1 norm a_i in $\boldsymbol{A}$ is associated with a lower individual flip rate ρ_i in $\boldsymbol{P}$. *The pseudocode for our noise generation is provided in Appendix E.*

Measuring the Change of the Average Disagreement via the Regression Coefficient To infer whether a dataset is causal or anticausal, the key is to determine whether there is a change in the average disagreement between pseudo labels (obtained through unsupervised methods) and modified labels (derived by injecting observed labels with increasing levels of noise). In causal scenarios, there should be no change, whereas in anticausal settings, a change is expected. Therefore, we inject different levels of label noise and measure the trend of disagreements as the level of injected label noise increases by employing a regression model.

To measure the disagreement, let $\boldsymbol{Y}'$ be the set containing pseudo labels for $\{\boldsymbol{x}_1, \boldsymbol{x}_2, \ldots, \boldsymbol{x}_m\}$. Let $\tilde{\boldsymbol{Y}}^\rho$ be the set of modified labels for $\{\boldsymbol{x}_1, \boldsymbol{x}_2, \ldots, \boldsymbol{x}_m\}$ after injecting instance-dependent noise with an expected noise level ρ. The disagreement between the pseudo-label set $\boldsymbol{Y}'$ and the modified label set $\tilde{\boldsymbol{Y}}^\rho$ is measured using the 0-1 loss, $\ell_{01} = \frac{\sum_{i=1}^m \mathbb{1}_{\{y'{}_i \neq \tilde{y}_i^\rho\}}}{m}$.

To measure the trend of the disagreement, we employ a linear regression model. Specifically, we *uniformly* sample 20 average noise levels from 0 to 0.5. We then inject label noise with each sampled averaged noise level (denoted as ρ^i) into the observed labels and calculate the average disagreement using the 0-1 loss. As a result, for each noise level ρ^i, a corresponding disagreement is calculated. Next, the linear regression model is employed to characterize the dependence between the noise level ρ and the loss ℓ_{01}. The objective is as follows.

$$\{\hat{\beta}_0, \hat{\beta}_1\} = \arg\min_{\beta_0, \beta_1} \frac{1}{n} \sum_{i=1}^{n} (\ell_{01}^i - (\beta_1 \rho^i + \beta_0))^2, \tag{2}$$

where $\hat{\beta}_0$, $\hat{\beta}_1$ refer to the estimated intercept and regression coefficient of the regression line, ℓ_{01}^i denotes $0-1$ loss calculated under the ρ^i noise level, respectively, and n is the total number of sampled noise levels. Accordingly, for causal datasets, the regression coefficient $\hat{\beta}_1$ should approximate 0. In contrast, for anticausal datasets, this regression coefficient should deviate significantly from 0.

A Hypothesis Test for the Regression Coefficient To rigorously validate the change of the disagreement, rather than directly evaluating if the regression coefficient $\hat{\beta}_1$ contained from Eq. (2)

[2] We have also tested different norms in our experiments, the influence is not large

is near 0, we perform the one-sample t-test to quantify whether the regression coefficient $\hat{\beta}_1$ is significantly different from zero. We repeat the entire procedure of sampling different noise levels, calculating disagreements, and performing linear regressions 30 times to obtain a set of regression coefficient values. These regression coefficient values are then utilized in our hypothesis test to verify if the average regression coefficient is significantly different from 0.

Let t^* be the observed value of the test statistic, P_0 denotes the t-distribution of the test statistic under the null hypothesis that the regression coefficient $\hat{\beta}_1$ is zero. Then the p-value of the t-test where $\hat{\beta}_1$ is significantly different from zero are as follows.

$$p = \mathbb{P}\left(T \geq t^* \mid T \sim P_0\right), \;\; t^* = \frac{\hat{\beta}_1 - 0}{\sqrt{\frac{1}{n-2}\frac{\sum_{i=1}^{n}\left(\ell_{01_i} - (\hat{\beta}_1\rho_i + \hat{\beta}_0)\right)^2}{\sum_{i=1}^{n}(\rho_i - \bar{\rho})^2}}/\sqrt{n}}.$$

We check whether the p-value is less than the significance level 0.05. If the condition holds, the null hypothesis will be rejected, indicating that the regression coefficient $\hat{\beta}_1$ is significantly different from zero, and the dataset is anticausal. Otherwise, the null hypothesis cannot be rejected, suggesting the regression coefficient $\hat{\beta}_1$ is zero. Then the dataset is very likely to be causal dataset.

3.3 Theoretical Analyses

We theoretically show that RoCA estimator holds the aforementioned asymmetric property, therefore it can detect causal and anticausal direction. Specifically, by applying RoCA estimator, under the causal setting, the disagreement and the noise level should not be dependent on each other, i.e., the regression coefficient β_1 is 0 in Theorem 1; under the anticausal setting, the disagreement and the noise level are dependent on each other, i.e., the regression coefficient β_1 is not 0 in Theorem 2.

Let $\mathcal{X}$ be the instance space and C the set of all possible classes. Let $S = \{(x_i, \tilde{y}_i)\}_{t=0}^{m}$ be an sample set. Let $h : \mathcal{X} \to \{1, \ldots, C\}$, be a hypothesis that predicts pseudo labels of instances. Concretely, it can be a K-means algorithm together with the Hungarian algorithm which matches the cluster ID to the corresponding pseudo labels. Let $\mathcal{H}$ be the hypothesis space, where $h \in \mathcal{H}$. Let $\tilde{R}^{\rho}(h) = \mathbb{E}_{(\boldsymbol{x},\tilde{y}^{\rho})\sim P(\boldsymbol{X},\tilde{Y}^{\rho})}[\mathbb{1}_{\{h(\boldsymbol{x})\neq\tilde{y}^{\rho}\}}]$ be the expected disagreement $\tilde{R}(h)$ between pseudo labels and generated labels $\tilde{y}^{\rho}$ with ρ-level noise injection. Let $\hat{\tilde{R}}_S^{\rho}(h)$ be the average disagreement (or empirical risk) of h on the set S after ρ-level noise injection. Theorem 1 and Theorem 2 leverage the concept of *empirical Rademacher complexity*, denoted as $\hat{\mathfrak{R}}_S(\mathcal{H})$ (Mohri et al., 2018).

Theorem 1 (Invariant Disagreements Under the Causal Settings)**.** *Under the causal setting, assume that for every instance and clean class pair (x, y), its observed label $\tilde{y}$ is obtained by a noise rate ρ_x such that $P(\tilde{Y} = \tilde{y}|Y = y, \boldsymbol{X} = x) = \frac{\rho_x}{C-1}$ for all $\tilde{y} \neq y \wedge \tilde{y} \in C$. Then after injecting noise to the sample with arbitrary average noise rates ρ^1 and ρ^2 such that $0 \leq \rho^1 \leq \rho^2 \leq 1$, with a $1 - \delta$ probability and $\delta > 0$,*

$$|\hat{\tilde{R}}_S^{\rho^1}(h) - \hat{\tilde{R}}_S^{\rho^2}(h)| \leq 4\hat{\mathfrak{R}}_S(\mathcal{H}) + 6\sqrt{\frac{\log\frac{4}{\delta}}{2m}}. \tag{3}$$

As the sample size m increases, the term $3\sqrt{\frac{\log\frac{4}{\delta}}{2m}}$ tends towards 0 at a rate of $\mathcal{O}(\frac{1}{\sqrt{m}})$. Additionally, the empirical Rademacher complexity $\hat{\mathfrak{R}}S(\mathcal{H})$ of the K-means algorithm also tends towards 0 at a rate of $\mathcal{O}(\frac{1}{\sqrt{m}})$, as demonstrated by Li & Liu (2021). Consequently, the right-hand side of Inequality (3) converges to 0 at a rate of $\mathcal{O}(\frac{1}{\sqrt{m}})$. This implies that with an increasing sample size, the difference between the disagreements $\hat{\tilde{R}}_S^{\rho^1}(h)$ and $\hat{\tilde{R}}_S^{\rho^2}(h)$, obtained by introducing different noise levels, will tend towards 0. In other words, the level of disagreement remains unaffected by changes in noise levels, consequently leading to the conclusion that the regression coefficient β_1 equals zero.

Theorem 2 (Variable Disagreements Under the Anticausal Setting)**.** *Under the anticausal setting, after injecting noise with a noise level $\rho = \mathbb{E}_X[\rho_x]$, $\tilde{R}^{\rho}(h) - \tilde{R}(h) = \mathbb{E}\left[\left(1 - \frac{C\tilde{R}(h,x)}{C-1}\right)\rho_x\right]$.*

Theorem 2 shows that the difference of the disagreements after noise injection between the disagreements on observed labels is $\mathbb{E}\left[\left(1 - \frac{C\tilde{R}(h,x)}{C-1}\right)\rho_x\right]$. Under the anticausal setting, the pseudo labels

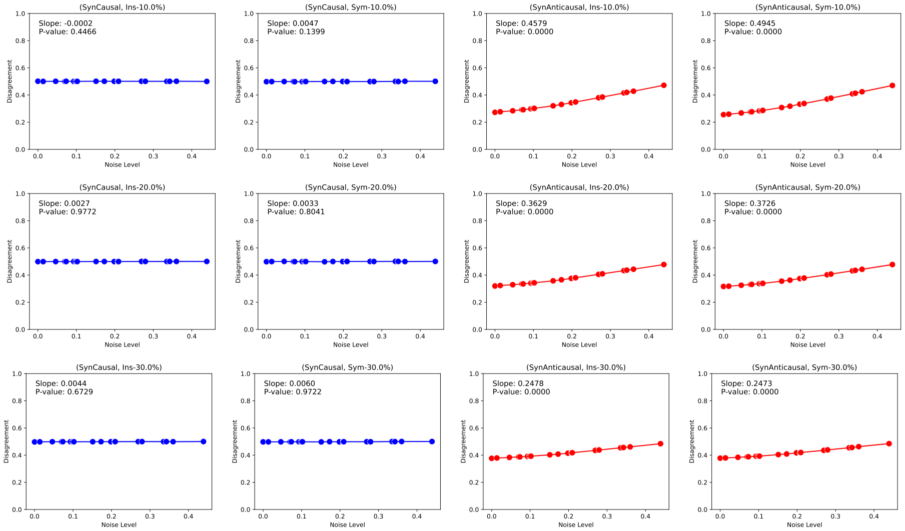

Figure 4: The change in the (average) disagreements and their standard deviations (which are minimal) between pseudo labels Y' and modified labels $\tilde{Y}^{\rho}$ with the increase in the noise level ρ for the synthetic datasets *synCausal* and *synAnticausal*.

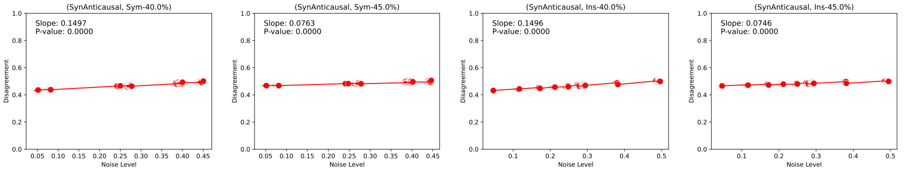

Figure 5: Performance of RoCA on the synAnticausal dataset when X and $\tilde{Y}$ have weak dependence

predicted by h are not random guesses. In this case, $\tilde{R}(h, x) \neq (C-1)/C$, then the difference is always nonzero. It implies that after injecting noise, the regression coefficient β_1 will be nonzero.

4 Experiments

We evaluated RoCA estimator across 22 datasets. This includes 2 synthetic datasets (*synCausal* and *synAnticausal*), 3 two-variate datasets (for checking pairwise causal relation with only two variables), 14 multi-variate datasets and 3 image datasets (*CIFAR10* (Krizhevsky et al., 2009), *CIFAR10N* (Wei et al., 2022), and *Clothing1M* (Xiao et al., 2015a)). Notably, *CIFAR10N* contains 5 real-world label-error settings named “Wors”, “Aggre”, “Random1”, “Random2”, and “Random3”. *Clothing1M* also contains real-world label errors and is a large-scale dataset with 1M images. We compare RoCA with 8 causal discovery methods. We use the K-means clustering method (Likas et al., 2003) for non-image datasets and the SPICE* clustering method (Niu et al., 2021) for image datasets to obtain the pseudo labels Y'. Our objective is to check if pseudo labels are random guesses of observed labels, so the number of pseudo labels matches the number of observed labels. Consequently, the cluster number is set to be identical to the number of observed labels.

To validate the robustness of RoCA estimator, different label errors are employed on synthetic datasets and non-image datasets: 1. **Symmetry Flipping** (Sym) (Patrini et al., 2017), which randomly replaces a percentage of labels in the training data with all possible labels. 2. **Pair Flipping** (Pair) (Han et al., 2018), where labels are only replaced by similar classes. For datasets with binary class labels, Sym and Pair noises are identical. 3. **Instance-Dependent Label Errors** (IDN) (Xia et al., 2020), where different instances have different transition matrices depending on parts of instances. To simulate scenarios with label errors, different errors are injected into the clean classes.

4.1 Experiments on Synthetic Datasets

We have generated two additional synthetic datasets, *synCausal* and *synAnticausal*, to validate our RoCA estimator. Each dataset consists of 20,000 instances with 5 attributes and 1 label. In the case

	SynCausal						
	0%	Ins-10%	Ins-20%	Ins-30%	Sym-10%	Sym-20%	Sym-30%
l_0	causal	causal	causal	causal	causal	causal	causal
l_2	causal	causal	causal	causal	causal	causal	causal
l_∞	causal	causal	causal	causal	causal	causal	causal

	SynAnticausal						
	0%	Ins-10%	Ins-20%	Ins-30%	Sym-10%	Sym-20%	Sym-30%
l_0	anticausal	anticausal	anticausal	anticausal	anticausal	anticausal	anticausal
l_2	anticausal	anticausal	anticausal	anticausal	anticausal	anticausal	anticausal
l_∞	anticausal	anticausal	anticausal	anticausal	anticausal	anticausal	anticausal

Table 1: Choice of norms for noise injection.

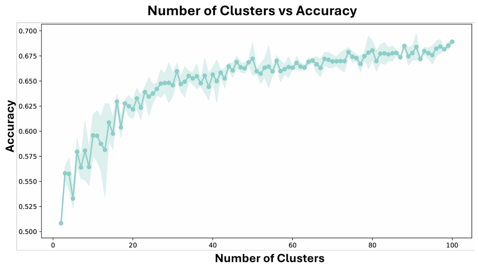

Figure 6: Effect for varying cluster numbers.

Table 2: Accuracy (%) for detecting the causal relation on different causal datasets.

	Accuracy (%) on Anticausal Datasets								
	GES	GIES	PC	ICD	RAI	FCI	LINGAM	CCDR	RoCA
SynAnticausal	**100.0**	**100.0**	**100.0**	**100.0**	0.0	**100.0**	0.0	70.0	**100.0**
WDBC	20.0	20.0	50.0	90.0	0.0	40.0	80.0	0.0	**100.0**
Letter	**100.0**	**100.0**	**100.0**	**100.0**	0.0	**100.0**	**100.0**	40.0	**100.0**
Breastcancer	40.0	40.0	40.0	70.0	60.0	70.0	0.0	30.0	**100.0**
Coil	80.0	80.0	10.0	0.0	0.0	90.0	**100.0**	0.0	**100.0**
G241C	70.0	70.0	**100.0**	0.0	0.0	**100.0**	50.0	90.0	**100.0**
Iris	10.0	10.0	40.0	50.0	**100.0**	50.0	0.0	70.0	**100.0**
Mushroom	**100.0**	**100.0**	90.0	0.0	0.0	0.0	0.0	0.0	70.0
Segment	90.0	90.0	90.0	**100.0**	0.0	**100.0**	0.0	80.0	**100.0**
Usps	50.0	50.0	20.0	0.0	0.0	90.0	**100.0**	0.0	**100.0**
Waveform	20.0	20.0	**100.0**	**100.0**	0.0	**100.0**	**100.0**	20.0	**100.0**
Digit1	20.0	20.0	40.0	0.0	0.0	**100.0**	**100.0**	**100.0**	**100.0**
Pair0047	40.0	40.0	NA	40.0	0.0	NA	0.0	0.0	**80.0**
Overall	56.9	56.9	65.0	50	12.3	78.3	48.5	41.7	**96.2**

Table 3: Accuracy (%) for detecting the anticausal relation on anticausal datasets.

	Accuracy (%) on Causal Datasets								
	GES	GIES	PC	ICD	RAI	FCI	LINGAM	CCDR	RoCA
SynCausal	70.0	70.0	40.0	0.0	**100.0**	0.0	**100.0**	**100.0**	**100.0**
Secstr	20.0	20.0	0.0	0.0	0.0	0.0	80.0	80.0	10.0
KrKp	0.0	0.0	30.0	10.0	0.0	0.0	0.0	40.0	**100.0**
Splice	0.0	0.0	0.0	0.0	0.0	0.0	0.0	0.0	**50.0**
Pair0070	0.0	0.0	NA	0.0	0.0	NA	0.0	0.0	**50.0**
Pair0071	0.0	0.0	NA	0.0	0.0	NA	0.0	0.0	0
Overall	15.0	15.0	17.5	1.7	16.7	0.0	30.6	36.7	**51.6**

of *synCausal*, we generate each instance by randomly sampling 5 values from a standard normal distribution to represent $\boldsymbol{X}$, and then compute the corresponding Y value using a polynomial function. This process simulates the data generative process where $\boldsymbol{X}$ causes Y. Conversely, the instances in *synAnticausal* are generated similarly, but in the opposite direction, to reflect that Y causes $\boldsymbol{X}$.

Validate Disagreement Change for Anticausal and Causal Cases Fig. 4 demonstrates the change of disagreement with 10%, 20% and 30% label errors for synCausal and synAnticausal datasets. For the *synCausal* dataset, the disagreement remains unchanged with the increase of noise rates, and the regression coefficient $\hat{\beta}_1$ of the regression line is close to 0. This is because Y' should be a random guess of noised $\tilde{Y}'$, which is proved in Theorem 1. On the other hand, for the *synAnticausal* dataset, there is a strong positive correlation between the disagreement and the noise level. In this case, Y' is well estimated, and both Y' and $\tilde{Y}$ are close to the latent (clean) class Y. When the noise level ρ of our injected noise is increased to 0.5, the modified label $\tilde{Y}^\rho$ becomes more seriously corrupted and tends to deviate far away from the observed label $\tilde{Y}$. This results in a larger disagreement between $\tilde{Y}^\rho$ and Y'. It is also observed that the regression coefficient becomes flattered when the label-error is larger (e.g., Ins-30% and Sym-30%). Under this circumstance, a large amount of original observable labels $\tilde{Y}$ are not identical to the latent clean class Y. Then $\tilde{Y}$ will be closer to a random guess of the clean class. Therefore the positive correlation between $\tilde{Y}$ and Y' becomes weak. However, in these extreme settings, our estimator is still robust, because the regression coefficient of our regression line is still significantly different from 0, and we can conclude that the dataset is anticausal.

Table 4: RoCA on large-scale noisy image datasets.

Clothing1M	*CIFAR10*	*CIFAR10N*				
		Worst	Aggre	Random1	Random2	Random3
$p = 0.0000$ **anticausal**	$p = 0.0000$ **anticausal**	$p = 0.0000$ **anticausal**	$p = 0.0000$ **anticausal**	$p = 0.0000$ **anticausal**	$p = 0.0000$ **anticausal**	$p = 0.0000$ **anticausal**

Robust to Label Errors Existing causal discovery methods primarily rely on checking the strength of dependence to infer causal relationships. Our method focuses on whether there is a change of dependence during the noise injection rather than the strength of the dependence. The strength of dependence can be easily influenced by label errors. As shown in the table in our appendix, with the increasing level of label errors, the performances of existing methods decrease. However, a consistent change of dependence can be observed (even if small) if $P(X)$ contains information about $P(\tilde{Y}|X)$. To further demonstrate this, we conducted additional experiments that let $P(X)$ and $P(\tilde{Y}|X)$ have very weak dependence on the anticausal dataset. This is achieved by manually adding high levels of label errors in $\tilde{Y}$ on the synthetic anticausal dataset. Specifically, we add 40% and 45% of label errors to synAnticausal dataset. Fig. 5 shows that despite the very small changes in dependence, with a regression coefficient (slope) such as 0.075, our method strongly rejects the null hypothesis that $P(X)$ does not contain information about $P(\tilde{Y}|X)$ with a p-value of 0.000.

Influence of Different Norms for Noise Injection We investigate the performance of RoCA when using different norms to generate instance-dependent label noise for our noise injection on synthetic causal and anticausal datasets. The observed label contains different types (symmetric, instance) and levels of label errors (10%, 20%, 30%). Fig. 1 shows that by changing the l_1 norm used in our paper to l_0, l_2, and l_∞. For all settings, changes in norms do not affect RoCA's prediction of whether the dataset is causal or anticausal. The table including p-values is left in our appendix.

Effect of Inconsistent Cluster Numbers We set the number of clusters equal to the number of different observed labels. Here, we show that making the number of clusters larger than the number of different observed labels results in unfaithful outcomes on SynCausal dataset. As shown in Fig. 6. The number of clusters and accuracy (1 - disagreements) are dependent. This contradicts the fact that $P(X)$ does not contain information about $P(\tilde{Y}|X)$. Intuitively, the reason is that in extreme cases, if the number of clusters equals the sample size, then the majority label within each cluster will be the observed label itself, and the accuracy will reach 100%.

4.2 Performance of RoCA on Real-World Datasets

We compare the RoCA method with other causal discovery algorithms in Table 2, Table 3 and Table 4. The accuracy (%) for detecting the anticausal relation on anticausal datasets is averaged over 10 different cases, including scenarios without label errors and those with different types of label errors (Instance 10%, Instance 20%, Instance 30%; Pair 10%, Pair 20%, Pair 30%; Sym 10%, Sym 20%, Sym 30%). We mark it as NA where the baseline cannot be employed to detect causal relations with only two variables. Notably, 1). the RoCA method is uniquely capable of being applied to large-scale image datasets *CIFAR10*, *CIFAR10N* and *Clothing1M*, which contain label errors, for the detection of causal and anticausal relations. The results demonstrate that our method is both accurate and robust. 2). For the *Pair0071* dataset, almost all methods misclassify it as an anticausal dataset. We believe this is due to the presence of a latent common cause affecting both the feature and the label. As acknowledged in their paper (Mooij et al., 2016), this scenario is possible.

5 Conclusion

This paper presents a scalable and robust estimator based on noise injection for determining causal and anticausal relations. The intuition is to leverage an information asymmetry between the distributions $P(\boldsymbol{X})$ and $P(\tilde{Y}|\boldsymbol{X})$ on anticausal and causal datasets. A practical estimator is proposed to check the asymmetric property. Our theoretical analyses and empirical results demonstrate the effectiveness of the RoCA estimator in determining the causal or anticausal relation of a dataset.

REFERENCES

Bryon Aragam and Qing Zhou. Concave penalized estimation of sparse gaussian bayesian networks. *The Journal of Machine Learning Research*, 16(1):2273–2328, 2015.

Zhitang Chen and Laiwan Chan. Causality in linear nongaussian acyclic models in the presence of latent gaussian confounders. *Neural Computation*, 25(6):1605–1641, 2013.

De Cheng, Tongliang Liu, Yixiong Ning, Nannan Wang, Bo Han, Gang Niu, Xinbo Gao, and Masashi Sugiyama. Instance-dependent label-noise learning with manifold-regularized transition matrix estimation. In *Proceedings of the IEEE/CVF Conference on Computer Vision and Pattern Recognition*, pp. 16630–16639, 2022.

D.M. Chickering. Optimal structure identification with greedy search. *Journal of Machine Learning Research*, 3(Nov), 2002.

Jia Deng, Wei Dong, Richard Socher, Li-Jia Li, Kai Li, and Li Fei-Fei. Imagenet: A large-scale hierarchical image database. In *2009 IEEE conference on computer vision and pattern recognition*, pp. 248–255. Ieee, 2009.

D. Geiger and D. Heckerman. Learning Gaussian networks. *Proceedings of the 10th Conference on Uncertainty in Artificial Intelligence*, 1994.

Aritra Ghosh and Andrew Lan. Contrastive learning improves model robustness under label noise. In *Proceedings of the IEEE/CVF Conference on Computer Vision and Pattern Recognition*, pp. 2703–2708, 2021.

P.D. Grünwald and P.M. Vitányi. *Handbook of the Philosophy of Information*, chapter Algorithms information theory. North Holland, 2008.

Bo Han, Quanming Yao, Xingrui Yu, Gang Niu, Miao Xu, Weihua Hu, Ivor Tsang, and Masashi Sugiyama. Co-teaching: Robust training of deep neural networks with extremely noisy labels. In *NeurIPS*, pp. 8527–8537, 2018.

Alain Hauser and Peter Bühlmann. Characterization and greedy learning of interventional markov equivalence classes of directed acyclic graphs. *The Journal of Machine Learning Research*, 13(1): 2409–2464, 2012.

D. Heckerman, D. Geiger, and D.M. Chickering. Learning Bayesian networks: the combination of knowledge and statistical data. *Machine Learning*, 20, 1995.

B. Huang, K. Zhang, Y. Lin, B. Schölkopf, and C. Glymour. Generalized score functions for causal discovery. *KDD*, 2018.

A. Hyvärinen and S.n.M. Smith. Pairwise likelihood ratios for estimation of non-gaussian structural equation models. *Journal of Machine Learning Research*, 14:111–152, 2013.

S. Imoto, T. Goto, and S. Miyano. Estimation of genetic networks and functional structures between genes by using Bayesian networks and nonparametric regression. *Pacific Symposium on Biocomputing*, (175-186), 2002.

D. Janzing and B. Schölkopf. Causal inference using the algorithmic Markov condition. *IEEE Transactions on Information Theory*, 56(10), 2010.

D. Janzing, J. Mooij, J. Zhang, K.and Lemeire, J. Zscheischler, P. Daniusis, B. Steudel, and B. Schölkopf. Information-geometric approach to inferring causal directions. *Artificial Intelligence*, 182-183, 2012.

Roy Jonker and Ton Volgenant. Improving the hungarian assignment algorithm. *Operations Research Letters*, 5(4):171–175, 1986.

D. Kalainathan, O. Goudet, I. Guyon, D. Lopez-Paz, and M. Sebag. Structural agnostic modeling: Adversarial learning of causal graphs. *arXiv:1803.04929v3*, 2020.

Mario Köppen. The curse of dimensionality. In *5th online world conference on soft computing in industrial applications (WSC5)*, volume 1, pp. 4–8, 2000.

Alex Krizhevsky, Geoffrey Hinton, et al. Learning multiple layers of features from tiny images. 2009.

Julius Kügelgen, Alexander Mey, Marco Loog, and Bernhard Schölkopf. Semi-supervised learning, causality, and the conditional cluster assumption. In *Conference on Uncertainty in Artificial Intelligence*, pp. 1–10. PMLR, 2020.

Alina Kuznetsova, Hassan Rom, Neil Alldrin, Jasper Uijlings, Ivan Krasin, Jordi Pont-Tuset, Shahab Kamali, Stefan Popov, Matteo Malloci, Alexander Kolesnikov, et al. The open images dataset v4. *International Journal of Computer Vision*, 128(7):1956–1981, 2020.

Michael S Lewicki and Terrence J Sejnowski. Learning overcomplete representations. *Neural computation*, 12(2):337–365, 2000.

Junnan Li, Richard Socher, and Steven CH Hoi. Dividemix: Learning with noisy labels as semi-supervised learning. In *ICLR*, 2019.

Shaojie Li and Yong Liu. Sharper generalization bounds for clustering. In *International Conference on Machine Learning*, pp. 6392–6402. PMLR, 2021.

Wen Li, Limin Wang, Wei Li, Eirikur Agustsson, and Luc Van Gool. Webvision database: Visual learning and understanding from web data. *arXiv preprint arXiv:1708.02862*, 2017.

Aristidis Likas, Nikos Vlassis, and Jakob J Verbeek. The global k-means clustering algorithm. *Pattern recognition*, 36(2):451–461, 2003.

Tongliang Liu and Dacheng Tao. Classification with noisy labels by importance reweighting. *IEEE Transactions on pattern analysis and machine intelligence*, 38(3):447–461, 2016.

Dhruv Mahajan, Ross Girshick, Vignesh Ramanathan, Kaiming He, Manohar Paluri, Yixuan Li, Ashwin Bharambe, and Laurens Van Der Maaten. Exploring the limits of weakly supervised pretraining. In *Proceedings of the European Conference on Computer Vision (ECCV)*, pp. 181–196, 2018.

Mehryar Mohri, Afshin Rostamizadeh, and Ameet Talwalkar. *Foundations of machine learning*. MIT press, 2018.

Joris M Mooij, Jonas Peters, Dominik Janzing, Jakob Zscheischler, and Bernhard Schölkopf. Distinguishing cause from effect using observational data: methods and benchmarks. *Journal of Machine Learning Research*, 17(32):1–102, 2016.

Chuang Niu, Hongming Shan, and Ge Wang. Spice: Semantic pseudo-labeling for image clustering. *arXiv preprint arXiv:2103.09382*, 2021.

Giorgio Patrini, Alessandro Rozza, Aditya Krishna Menon, Richard Nock, and Lizhen Qu. Making deep neural networks robust to label noise: A loss correction approach. In *CVPR*, pp. 1944–1952, 2017.

J. Pearl. *Causality: Models, Reasoning, and Inference*. Cambridge University Press, New York, NY, USA, 2000. ISBN 0-521-77362-8.

J Peters, JM Mooij, D Janzing, and B Schölkopf. Causal discovery with continuous additive noise models. *Journal of Machine Learning Research*, 15(1):2009–2053, 2014.

J. Peters, D. Janzing, and B. Scholkopf. *Elements of Causal Inference*. MIT Press, Cambridge, Massachusetts, 2017a.

Jonas Peters, Dominik Janzing, and Bernhard Scholkopf. Causal inference on discrete data using additive noise models. *IEEE Transactions on Pattern Analysis and Machine Intelligence*, 33(12): 2436–2450, 2011.

Jonas Peters, Dominik Janzing, and Bernhard Schölkopf. *Elements of causal inference: foundations and learning algorithms*. The MIT Press, 2017b.

Raanan Y Rohekar, Shami Nisimov, Yaniv Gurwicz, and Gal Novik. Iterative causal discovery in the possible presence of latent confounders and selection bias. *Advances in Neural Information Processing Systems*, 34:2454–2465, 2021.

B Schölkopf, D Janzing, J Peters, E Sgouritsa, K Zhang, and J Mooij. On causal and anticausal learning. In *29th International Conference on Machine Learning (ICML 2012)*, pp. 1255–1262. International Machine Learning Society, 2012.

Bernhard Schölkopf, Francesco Locatello, Stefan Bauer, Nan Rosemary Ke, Nal Kalchbrenner, Anirudh Goyal, and Yoshua Bengio. Toward causal representation learning. *Proceedings of the IEEE*, 109(5):612–634, 2021.

Clayton Scott, Gilles Blanchard, and Gregory Handy. Classification with asymmetric label noise: Consistency and maximal denoising. In *COLT*, pp. 489–511, 2013.

R. D. Shah and J. Peters. The hardness of conditional independence testing and the generalised covariance measure. *The Annals of Statistics*, 48(3), 2020.

Shohei Shimizu, Patrik O Hoyer, Aapo Hyvärinen, Antti Kerminen, and Michael Jordan. A linear non-gaussian acyclic model for causal discovery. *Journal of Machine Learning Research*, 7(10), 2006.

Shohei Shimizu, Takanori Inazumi, Yasuhiro Sogawa, Aapo Hyvärinen, Yoshinobu Kawahara, Takashi Washio, Patrik O Hoyer, and Kenneth Bollen. DirectLiNGAM: A direct method for learning a linear non-Gaussian structural equation model. *Journal of Machine Learning Research*, 12(Apr):1225–1248, 2011.

P. Spirtes, C. Glymour, and R. Scheines. *Causation, prediction, and search*. MIT Press, Cambridge, Massachusetts, 2nd edition, 2000a.

Peter Spirtes, Clark N Glymour, Richard Scheines, and David Heckerman. *Causation, prediction, and search*. MIT press, 2000b.

Tatsuya Tashiro, Shohei Shimizu, Aapo Hyvärinen, and Takashi Washio. Parcelingam: A causal ordering method robust against latent confounders. *Neural computation*, 26(1):57–83, 2014.

Wouter Van Gansbeke, Simon Vandenhende, Stamatios Georgoulis, Marc Proesmans, and Luc Van Gool. Scan: Learning to classify images without labels. In *European Conference on Computer Vision*, pp. 268–285. Springer, 2020.

Yisen Wang, Xingjun Ma, Zaiyi Chen, Yuan Luo, Jinfeng Yi, and James Bailey. Symmetric cross entropy for robust learning with noisy labels. In *Proceedings of the IEEE/CVF international conference on computer vision*, pp. 322–330, 2019.

Jiaheng Wei, Zhaowei Zhu, Hao Cheng, Tongliang Liu, Gang Niu, and Yang Liu. Learning with noisy labels revisited: A study using real-world human annotations. In *The Tenth International Conference on Learning Representations, ICLR 2022, Virtual Event, April 25-29, 2022*. OpenReview.net, 2022.

Xiaobo Xia, Tongliang Liu, Bo Han, Nannan Wang, Mingming Gong, Haifeng Liu, Gang Niu, Dacheng Tao, and Masashi Sugiyama. Part-dependent label noise: Towards instance-dependent label noise. *NerurIPS*, 2020.

Tong Xiao, Tian Xia, Yi Yang, Chang Huang, and Xiaogang Wang. Learning from massive noisy labeled data for image classification. In *IEEE Conference on Computer Vision and Pattern Recognition, CVPR 2015, Boston, MA, USA, June 7-12, 2015*, pp. 2691–2699. IEEE Computer Society, 2015a. doi: 10.1109/CVPR.2015.7298885.

Tong Xiao, Tian Xia, Yi Yang, Chang Huang, and Xiaogang Wang. Learning from massive noisy labeled data for image classification. In *CVPR*, pp. 2691–2699, 2015b.

Raanan Yehezkel and Boaz Lerner. Bayesian network structure learning by recursive autonomy identification. *Journal of Machine Learning Research*, 10(7), 2009.

Alessio Zanga, Elif Ozkirimli, and Fabio Stella. A survey on causal discovery: Theory and practice. *International Journal of Approximate Reasoning*, 151:101–129, 2022.

Kun Zhang and Aapo Hyvarinen. On the identifiability of the post-nonlinear causal model. In *Conference on Uncertainty in Artificial Intelligence*, 2009.

Appendix

Table of Contents

A A Review of Causal Discovery Methods

Constraint-Based and Score-Based Approaches. To build a graph that captures these conditional independencies, the majority of constraint-based techniques look for conditional independencies in the empirical joint distribution. Since numerous graphs frequently satisfy a given set of conditional dependencies, as was discussed above, constraint-based methods frequently produce a graph that represents some Markov equivalence classes. Unfortunately, large sample sizes are necessary for conditional independence tests to be reliable, and (Shah & Peters, 2020) highlights further difficulties in controlling Type I errors.

Score-based approaches test the validity of a candidate graph $\mathcal{G}$ according to some scoring function S. The goal is therefore stated as (Peters et al., 2017a):

$$\hat{\mathcal{G}} = \text{argmax}_{\mathcal{G} \text{ over } \mathbf{X}} S(\mathcal{D}, \mathcal{G}) \tag{4}$$

where the empirical data for the variables $\mathbf{X}$ is represented by $\mathcal{D}$. Common scoring functions include the Bayesian Information Criterion (BIC) (Geiger & Heckerman, 1994), the Minimum Description Length (as an approximation of Kolmogorov Complexity) (Janzing & Schölkopf, 2010; Grünwald & Vitányi, 2008; Kalainathan et al., 2020), the Bayesian Gaussian equivalent (BGe) score (Geiger & Heckerman, 1994), the Bayesian Dirichlet equivalence (BDe) score (Heckerman et al., 1995), the Bayesian Dirichlet equivalence uniform (BDeu) score (Heckerman et al., 1995), and others (Imoto et al., 2002; Hyvärinen & Smith, 2013; Huang et al., 2018).

Functional Causal Models. Methods based on causal function provide an alternate strategy for estimating causal effects. Assumptions about the data generation process are used in these causal function-based techniques. The causal function-based approach fits the causal function model among variables and then infers causal directions using causal assumptions, such as a non-Gaussian assumption of the noise (Shimizu et al., 2006; 2011) the independence assumption between cause variables and noise (Zhang & Hyvarinen, 2009; Peters et al., 2011; 2014) and the independence assumption between the distribution of cause variables and the causal function (Janzing et al., 2012). Most LiNGAM-based approaches for the linear case (Shimizu et al., 2006) assume non-Gaussian noise and linear causal relations between variables. This model seeks to determine a causal order among the random observed variables.

To deal with linear latent confounders, an estimation method utilizing overcomplete ICA (Lewicki & Sejnowski, 2000) is suggested. However, overcomplete ICA algorithms usually suffer from local optimum and cannot be employed when the number of variables is large.

By evaluating the independence between the estimated exogenous variables and the residual, (Tashiro et al., 2014) identify latent confounders. They discover that variables from subsets that are not impacted by latent confounders are included, and they estimate causal orders one at a time. (Chen & Chan, 2013) investigate linear non-Gaussian acyclic models in the presence of latent Gaussian confounders (LiNGAM-GC), which assumes that the latent confounders are Gaussian distributed independently.

B Causal Graphs and Structural Causal Models (SCM)

Directed acyclic graphs (DAGs) serve as a formalism for representing causal relationships. In these graphs, arrows point from the parent node (direct cause) to the child node (direct effect) (Pearl, 2000). Building upon this graphical representation, a structural causal model (SCM) can be constructed to capture the causal mechanisms that underlie the data distribution.

An SCM is composed of a set of variables interconnected by functions, representing the flow of information. This model elucidates the causal relationships among variables, offering a detailed insight into the data generation process. Consider a DAG $G = (V, E)$ defined over a set of variables $\{X_1, X_2, \cdots, X_d, Y\}$, with P representing their joint distribution. Let $\boldsymbol{X}$ be the set $\{X_1, X_2, \cdots, X_d\}$. The notation $\boldsymbol{X}_{PA_i^G}$ refers to the direct causes of X_i, while $\boldsymbol{Y}_{PA^G}$ denotes the direct causes of Y. Disturbances or errors in the generative processes of X_i and Y are represented by N_i and N_y, respectively. The SCM for a classification dataset can be expressed as:

$$X_i := f_i(\boldsymbol{X}_{PA_i^G}, N_i), \ \ i = 1, ..., d; \ Y := f_y(\boldsymbol{Y}_{PA^G}, N_y).$$

The causal factorization of the joint distribution is given by:

$$P(\boldsymbol{X}, Y) = P(Y|\boldsymbol{Y}_{PA^G}) \prod_i P(X_i|\boldsymbol{X}_{PA_i^G}). \tag{5}$$

It's worth noting that both $\boldsymbol{X}_{PA_i^G}$ and $\boldsymbol{Y}_{PA^G}$ are allowed to be empty sets.

C Understanding the Independence between Distributions

To concretely explain what is meant by $P(\boldsymbol{X})$ not being useful for predicting class Y, let's consider an illustrative example that follows the generative process of causal datasets.

- We act as the data collector. 1). we randomly sample a photo $\boldsymbol{X}$ from Instagram.
- Let Tom be the annotator. He will annotate each $\boldsymbol{X}$ we pass but without any knowledge of $P(\boldsymbol{X})$.
- Following the generative process, 2). we pass the photo $\boldsymbol{X}$ to Tom. Tom writes the label Y on the back of the photo $\boldsymbol{X}$ and puts the photo in a black box.
- We repeat the process 1), and Tom repeats the process 2).

The question then arises: *can we act like a clustering algorithm by looking at $P(\boldsymbol{X})$ to understand how photos in the box are labeled?* Generally, the answer is no. Intuitively, there are too many possible ways to annotate the photo. Tom could label the photos based on whether the image contains a human, the number of humans, night vs. day, and other characteristics. We have no idea about his mechanism by only looking at $P(\boldsymbol{X})$. In this case, $P(\boldsymbol{X})$ does not inform $P(Y|\boldsymbol{X})$.

D More Experiments

D.1 Introduction of Real-world Causal Datasets

1. *KrKp* dataset contains 3196 instances with 36 attributes. Each instance is a board description for the chess endgame, where the feature attributes describe the board and the label determines whether it is ”win” or ”nowin”. It is considered a causal dataset since the board description causally influences whether white will win.
2. *Splice* dataset contains 3190 instances with 60 attributes, where attributes describe sequential DNA nucleotide positions and the label is the type of splice sites. It is considered a causal dataset since the DNA sequence causes the splice sites.
3. *SecStr* dataset contains 83680 instances with 15 attributes, where attributes describe the amino acid and the label is the corresponding secondary chemical structure. It is considered a causal dataset since the secondary structure is determined by its amino acid features.
4. *Pair0070* dataset contains 4499 instances. It is a bi-variate dataset, where the feature describes parameters and the label contains the corresponding answers.It is considered as a causal dataset since parameters determine the answers.
5. *Pair0071* dataset contains 120 instances. It is a bi-variate dataset, where the feature describes symptoms and the label contains the corresponding classification of diseases. It is considered as a causal dataset since symptoms determine the type of diseases.

D.2 Introduction of Real-world Anticausal Datasets

1. *WDBC* dataset contains 569 instances with 32 attributes. It is an anticausal dataset, where the class causes some of the tumor features.
2. *Letter* dataset contains 20000 instances with 16 attributes. It is an anticausal daset, where the class (letter) causes the produced image of the letter.
3. *Breastcancer* dataset contains 286 instances with 9 attributes. It is an anticausal dataset, where the class causes some of the tumor features.
4. *Coil* dataset contains 1500 instances with 241 attributes. It is considered an anticausal/confounded dataset because the six-state class and the features are confounded by the 24-state variable of all objects.
5. *G241C* dataset contains 1500 instances with 241 attributes. It is considered an anticausal dataset since the class determines the features.
6. *Iris* dataset contains 150 instances with 4 attributes. It is an anticausal dataset, where the size of the plant is an effect of the category.
7. *Mushroom* dataset contains 8124 instances with 22 attributes. It is an anticausal dataset, where the attributes of the mushroom and the class are confounded by the mushroom taxonomy.
8. *Segment* dataset contains 2310 instances with 19 attributes. It is an anticausal dataset, where the class causes the features of the image.
9. *Usps* dataset contains 1500 instances with 240 attributes. It is an anticausal dataset, where the class and the features are confounded by the 10-state variable of all digits.
10. *Waveform* dataset contains 5000 instances with 21 attributes attributes and 1 label. Each class is generated from a combination of 2 or 3 ”base” waves. It is considered an anticausal dataset since the class of the wave causes its attributes.
11. *Pair0047* dataset contains 255 instances. It is a bi-variate dataset, where the feature describes the number of cars and the label contains the type of day. It is considered as a causal dataset since number of cars determine the type of day.
12. *CIFAR10* dataset contains 60000 32×32 color images (attributes) in 10 classes (label), with 6000 images per class. It is considered an anticausal dataset since the images are collected according to the predefined 10 different labels.
13. *CIFAR10N* has the same number of instances and attributes as those of *CIFAR10* while there are 5 different types of human-annotated real-world noisy labels from Amazon Mechanical Turk.

14. *Clothing1M* contains 1M clothing images in 14 classes. It is a causal dataset with noisy labels since the image determines its class and the data is collected from several online shopping websites.
15. *Digit1* dataset contains 1500 instances with 241 attributes. It is considered an anticausal dataset because the positive or negative angle and the features are confounded by the variable of continuous angle.

D.3 Introduction of Baseline Causal Discovery Methods

The baseline causal discovery methods we employed are as follows.

1. GES (Chickering, 2002): The Greedy Equivalence Search algorithm is a score-based Bayesian approach that heuristically searches for a graph that minimizes a likelihood score on the given data.
2. GIES (Hauser & Bühlmann, 2012): The Greedy Interventional Equivalence Search algorithm is similar to GES, but it incorporates interventional data for inference.
3. PC (Spirtes et al., 2000b): The Peter-Clark algorithm is one of the renowned score-based methods for causal discovery. It efficiently employs conditional tests on variables and variable sets.
4. ICD (Rohekar et al., 2021): Iterative Causal Discovery recovers causal graphs in the presence of latent confounders and selection bias. ICD relies on the causal Markov and faithfulness assumptions and identifies the equivalence class of the underlying causal graph.
5. RAI (Yehezkel & Lerner, 2009): Recursive Autonomy Identification learns the structure by sequentially applying conditional independence tests, edge direction, and structure decomposition into autonomous sub-structures.
6. FCI (Spirtes et al., 2000a): Fast Causal Inference stands out among constraint-based methods for its ability to detect latent confounders.
7. LiNGAM (Shimizu et al., 2006): Linear Non-Gaussian Acyclic Model assumes that there are no hidden confounders and all of the error terms are non-gaussian and detects causal relationships from observed data accordingly.
8. CCDR (Aragam & Zhou, 2015): Concave Penalized Coordinate Descent with Reparametrization is a fast, score-based method for learning Bayesian networks, utilizing sparse regularization and block-cyclic coordinate descent.

D.4 More Experiments on Real-world Datasets

In Table 5 and 6, we present the results of causal discovery obtained using our RoCA estimator compared to other baseline methods. Our RoCA estimator outperforms the baseline methods in accurately identifying the causal relationships. Among the 14 of 16 datasets, our RoCA estimator correctly identified the causal relationship between X and Y in the majority of cases. This holds even when the datasets contained different types of label noise, such as instance-dependent, pair, and symmetric noise, with noise rates ranging from 0% to 30%. On the other hand, the performance of the baseline methods was generally satisfactory for anticausal datasets but lacked accuracy when dealing with causal datasets. This is because a causal dataset requires no features in X to cause Y, which presents a challenge for these baseline methods. They need to ensure that there is no edge from any vertex representing features in X pointing to the vertex representing Y when recovering the causal diagram. Although these baseline methods tend to perform well in general tasks, they may not be suitable for this particular task, leading to misclassification of datasets as anticausal.

Furthermore, the time complexity of some baseline methods hinders their application to datasets with a large number of features, such as image datasets or datasets with hundreds of features (e.g., *G241C*, *Coil*, etc.). Completing the algorithm within a reasonable time frame becomes challenging for these methods. In this case, we classify the results as unknown.

Table 5: Comparing with baselines on synthetic and real-world datasets (cont.).

	Method	Original	Instance			Pair			Sym		
		0%	10%	20%	30%	10%	20%	30%	10%	20%	30%
Pair0070 (causal)	GES	unknown	unknown	unknown	unknown	unknown	unknown	unknown	unknown	unknown	unknown
	GIES	unknown	unknown	unknown	unknown	unknown	unknown	unknown	unknown	unknown	unknown
	ICD	unknown	unknown	unknown	unknown	unknown	unknown	unknown	unknown	unknown	unknown
	RAI	unknown	unknown	unknown	unknown	unknown	unknown	unknown	unknown	unknown	unknown
	CCDR	unknown	unknown	unknown	unknown	unknown	unknown	unknown	unknown	unknown	unknown
	Our method	p=0.0463 anticausal	p=0.9966 **causal**	p=0.8995 **causal**	p=0.1843 **causal**	p=0.1791 **causal**	p=0.0000 anticausal	p=0.0158 anticausal	p=0.1791 **causal**	p=0.0000 anticausal	p=0.0158 anticausal
Pair0071 (causal)	GES	anticausal	anticausal	anticausal	anticausal	anticausal	anticausal	anticausal	anticausal	anticausal	anticausal
	GIES	anticausal	anticausal	anticausal	anticausal	anticausal	anticausal	anticausal	anticausal	anticausal	anticausal
	ICD	anticausal	anticausal	anticausal	anticausal	anticausal	anticausal	unknown	anticausal	anticausal	unknown
	RAI	anticausal	anticausal	anticausal	anticausal	anticausal	anticausal	anticausal	anticausal	anticausal	anticausal
	LINGAM	unknown	unknown	unknown	unknown	unknown	unknown	unknown	unknown	unknown	unknown
	CCDR	anticausal	anticausal	anticausal	anticausal	anticausal	anticausal	anticausal	anticausal	anticausal	anticausal
	Our method	p=0.0007 anticausal	p=0.0000 anticausal	p=0.0000 anticausal	p=0.0001 anticausal	p=0.0197 anticausal	p=0.0000 anticausal	p=0.0000 anticausal	p=0.0000 anticausal	p=0.0000 anticausal	p=0.0000 anticausal
SynAnticausal (anticausal)	GES	**anticausal**	**anticausal**	**anticausal**	**anticausal**	**anticausal**	**anticausal**	**anticausal**	**anticausal**	**anticausal**	**anticausal**
	GIES	**anticausal**	**anticausal**	**anticausal**	**anticausal**	**anticausal**	**anticausal**	**anticausal**	**anticausal**	**anticausal**	**anticausal**
	PC	**anticausal**	**anticausal**	**anticausal**	**anticausal**	**anticausal**	**anticausal**	**anticausal**	**anticausal**	**anticausal**	**anticausal**
	ICD	**anticausal**	**anticausal**	**anticausal**	**anticausal**	**anticausal**	**anticausal**	**anticausal**	**anticausal**	**anticausal**	**anticausal**
	RAI	causal	causal	causal	causal	causal	causal	causal	causal	causal	causal
	FCI	**anticausal**	**anticausal**	**anticausal**	**anticausal**	**anticausal**	**anticausal**	**anticausal**	**anticausal**	**anticausal**	**anticausal**
	LINGAM	unknown	unknown	unknown	unknown	unknown	unknown	unknown	unknown	unknown	unknown
	CCDR	**anticausal**	**anticausal**	**anticausal**	causal	**anticausal**	**anticausal**	causal	**anticausal**	**anticausal**	causal
	Our method	p=0.0000 **anticausal**	p=0.0000 **anticausal**	p=0.0000 **anticausal**	p=0.0000 **anticausal**	p=0.0000 **anticausal**	p=0.0000 **anticausal**	p=0.0000 **anticausal**	p=0.0000 **anticausal**	p=0.0000 **anticausal**	p=0.0000 **anticausal**
WDBC (anticausal)	GES	**anticausal**	causal	causal	causal	causal	causal	causal	causal	**anticausal**	causal
	GIES	**anticausal**	causal	causal	causal	causal	causal	causal	causal	**anticausal**	causal
	PC	**anticausal**	**anticausal**	**anticausal**	unknown	**anticausal**	unknown	unknown	**anticausal**	unknown	unknown
	ICD	**anticausal**	**anticausal**	**anticausal**	unknown	**anticausal**	**anticausal**	**anticausal**	**anticausal**	**anticausal**	**anticausal**
	RAI	unknown	unknown	unknown	unknown	unknown	unknown	unknown	unknown	unknown	unknown
	FCI	**anticausal**	**anticausal**	unknown	unknown	**anticausal**	unknown	unknown	**anticausal**	unknown	unknown
	LINGAM	**anticausal**	unknown	unknown	unknown	unknown	unknown	unknown	**anticausal**	unknown	unknown
	CCDR	causal	causal	causal	causal	causal	causal	causal	causal	causal	causal
	Our method	p=0.0000 **anticausal**	p=0.0000 **anticausal**	p=0.0000 **anticausal**	p=0.0000 **anticausal**	p=0.0000 **anticausal**	p=0.0000 **anticausal**	p=0.0000 **anticausal**	p=0.0000 **anticausal**	p=0.0000 **anticausal**	p=0.0000 **anticausal**
Letter (anticausal)	GES	**anticausal**	**anticausal**	**anticausal**	**anticausal**	**anticausal**	**anticausal**	**anticausal**	**anticausal**	**anticausal**	**anticausal**
	GIES	**anticausal**	**anticausal**	**anticausal**	**anticausal**	**anticausal**	**anticausal**	**anticausal**	**anticausal**	**anticausal**	**anticausal**
	PC	**anticausal**	**anticausal**	**anticausal**	**anticausal**	**anticausal**	**anticausal**	**anticausal**	**anticausal**	**anticausal**	**anticausal**
	ICD	**anticausal**	**anticausal**	**anticausal**	**anticausal**	**anticausal**	**anticausal**	**anticausal**	**anticausal**	**anticausal**	**anticausal**
	RAI	unknown	unknown	unknown	unknown	unknown	unknown	unknown	unknown	unknown	unknown
	FCI	**anticausal**	**anticausal**	**anticausal**	**anticausal**	**anticausal**	**anticausal**	**anticausal**	**anticausal**	**anticausal**	**anticausal**
	LINGAM	**anticausal**	**anticausal**	**anticausal**	**anticausal**	**anticausal**	**anticausal**	**anticausal**	**anticausal**	**anticausal**	**anticausal**
	CCDR	unkown	unkown	causal	causal	**anticausal**	**anticausal**	causal	**anticausal**	unknown	**anticausal**
	Our method	p=0.0000 **anticausal**	p=0.0000 **anticausal**	p=0.0000 **anticausal**	p=0.0000 **anticausal**	p=0.0000 **anticausal**	p=0.0000 **anticausal**	p=0.0000 **anticausal**	p=0.0000 **anticausal**	p=0.0000 **anticausal**	p=0.0000 **anticausal**
Breastcancer (anticausal)	GES	**anticausal**	unknown	**anticausal**	unknown	unknown	**anticausal**	unknown	unknown	**anticausal**	unknown
	GIES	**anticausal**	unknown	**anticausal**	unknown	unknown	**anticausal**	unknown	unknown	**anticausal**	unknown
	PC	**anticausal**	unknown	**anticausal**	unknown	unknown	**anticausal**	unknown	unknown	**anticausal**	unknown
	ICD	**anticausal**	**anticausal**	**anticausal**	unknown	**anticausal**	**anticausal**	unknown	**anticausal**	**anticausal**	unknown
	RAI	**anticausal**	**anticausal**	**anticausal**	**anticausal**	**anticausal**	unknown	unknown	**anticausal**	unknown	unknown
	FCI	**anticausal**	**anticausal**	**anticausal**	unknown	**anticausal**	**anticausal**	unknown	**anticausal**	**anticausal**	unknown
	LINGAM	unknown	unknown	unknown	unknown	unknown	unknown	unknown	unknown	unknown	unknown
	CCDR	causal	causal	causal	**anticausal**	causal	causal	**anticausal**	causal	causal	**anticausal**
	Our method	p=0.0000 **anticausal**	p=0.0000 **anticausal**	p=0.0000 **anticausal**	p=0.0000 **anticausal**	p=0.0000 **anticausal**	p=0.0000 **anticausal**	p=0.0000 **anticausal**	p=0.0000 **anticausal**	p=0.0000 **anticausal**	p=0.0000 **anticausal**
Coil (anticausal)	GES	**anticausal**	causal	**anticausal**	**anticausal**	**anticausal**	causal	**anticausal**	**anticausal**	**anticausal**	**anticausal**
	GIES	**anticausal**	causal	**anticausal**	**anticausal**	**anticausal**	causal	**anticausal**	**anticausal**	**anticausal**	**anticausal**
	PC	causal	unknown	causal	unknown	unknown	**anticausal**	causal	causal	unknown	unknown
	ICD	unknown	unknown	unknown	unknown	unknown	unknown	unknown	unknown	unknown	unknown
	RAI	unknown	unknown	unknown	unknown	unknown	unknown	unknown	unknown	unknown	unknown
	FCI	**anticausal**	**anticausal**	**anticausal**	unknown	**anticausal**	**anticausal**	**anticausal**	**anticausal**	**anticausal**	**anticausal**
	LINGAM	**anticausal**	**anticausal**	**anticausal**	**anticausal**	**anticausal**	**anticausal**	**anticausal**	**anticausal**	**anticausal**	**anticausal**
	CCDR	causal	causal	unknown	unknown	causal	causal	causal	causal	causal	causal
	Our method	p=0.0000 **anticausal**	p=0.0000 **anticausal**	p=0.0000 **anticausal**	p=0.0000 **anticausal**	p=0.0000 **anticausal**	p=0.0000 **anticausal**	p=0.0000 **anticausal**	p=0.0000 **anticausal**	p=0.0000 **anticausal**	p=0.0000 **anticausal**
G241C (anticausal)	GES	**anticausal**	**anticausal**	**anticausal**	**anticausal**	**anticausal**	**anticausal**	**anticausal**	causal	causal	causal
	GIES	**anticausal**	**anticausal**	**anticausal**	**anticausal**	**anticausal**	**anticausal**	**anticausal**	causal	causal	causal
	PC	**anticausal**	**anticausal**	unknown	**anticausal**	**anticausal**	**anticausal**	**anticausal**	**anticausal**	**anticausal**	**anticausal**
	ICD	unknown	unknown	unknown	unknown	unknown	unknown	unknown	unknown	unknown	unknown
	RAI	unknown	unknown	unknown	unknown	unknown	unknown	unknown	unknown	unknown	unknown
	FCI	**anticausal**	**anticausal**	**anticausal**	**anticausal**	**anticausal**	**anticausal**	**anticausal**	**anticausal**	**anticausal**	**anticausal**
	LINGAM	**anticausal**	unknown	causal	unknown	**anticausal**	causal	**anticausal**	unknown	**anticausal**	**anticausal**
	CCDR	**anticausal**	**anticausal**	**anticausal**	**anticausal**	**anticausal**	**anticausal**	**anticausal**	**anticausal**	causal	**anticausal**
	Our method	p=0.0000 **anticausal**	p=0.0000 **anticausal**	p=0.0000 **anticausal**	p=0.0000 **anticausal**	p=0.0000 **anticausal**	p=0.0000 **anticausal**	p=0.0000 **anticausal**	p=0.0000 **anticausal**	p=0.0000 **anticausal**	p=0.0000 **anticausal**

Table 6: Comparing with baselines on synthetic and real-world datasets.

	Method	Original	Instance			Pair			Sym		
		0%	10%	20%	30%	10%	20%	30%	10%	20%	30%
Iris (anticausal)	GES	**anticausal**	unknown	unknown	unknown	unknown	unknown	unknown	unknown	unknown	unknown
	GIES	**anticausal**	unknown	unknown	unknown	unknown	unknown	unknown	unknown	unknown	unknown
	PC	**anticausal**	unknown	**anticausal**	unknown	**anticausal**	unknown	unknown	**anticausal**	causal	unknown
	ICD	**anticausal**	unknown	**anticausal**	unknown	**anticausal**	unknown	unknown	**anticausal**	**anticausal**	unknown
	RAI	**anticausal**	**anticausal**	**anticausal**	**anticausal**	**anticausal**	**anticausal**	**anticausal**	**anticausal**	**anticausal**	**anticausal**
	FCI	**anticausal**	unknown	**anticausal**	unknown	**anticausal**	unknown	unknown	**anticausal**	**anticausal**	unknown
	LINGAM	unknown	unknown	unknown	unknown	unknown	unknown	unknown	unknown	unknown	unknown
	CCDR	**anticausal**	**anticausal**	**anticausal**	causal	**anticausal**	causal	causal	**anticausal**	**anticausal**	**anticausal**
	Our method	p=0.0000 **anticausal**	p=0.0000 **anticausal**	p=0.0000 **anticausal**	p=0.0000 **anticausal**	p=0.0000 **anticausal**	p=0.0000 **anticausal**	p=0.0000 **anticausal**	p=0.0000 **anticausal**	p=0.0000 **anticausal**	p=0.0000 **anticausal**
Mushroom	GES	**anticausal**	**anticausal**	**anticausal**	**anticausal**	**anticausal**	**anticausal**	**anticausal**	**anticausal**	**anticausal**	**anticausal**
	GIES	**anticausal**	**anticausal**	**anticausal**	**anticausal**	**anticausal**	**anticausal**	**anticausal**	**anticausal**	**anticausal**	**anticausal**
	PC	causal	**anticausal**	**anticausal**	**anticausal**	**anticausal**	**anticausal**	**anticausal**	**anticausal**	**anticausal**	**anticausal**
	ICD	unknown	unknown	unknown	unknown	unknown	unknown	unknown	unknown	unknown	unknown
	RAI	unknown	unknown	unknown	unknown	unknown	unknown	unknown	unknown	unknown	unknown
	LINGAM	unknown	unknown	unknown	unknown	unknown	unknown	unknown	unknown	unknown	unknown
	CCDR	unknown	unknown	unknown	unknown	unknown	unknown	unknown	unknown	unknown	unknown
	Our method	p=0.0000 **anticausal**	p=0.2127 causal	p=0.0000 **anticausal**	p=0.0000 **anticausal**	p=0.0000 **anticausal**	p=0.0000 **anticausal**	p=0.0865 causal	p=0.0000 **anticausal**	p=0.0000 **anticausal**	p=0.0865 causal
Segment (anticausal)	GES	unknown	**anticausal**	**anticausal**	**anticausal**	**anticausal**	**anticausal**	**anticausal**	**anticausal**	**anticausal**	**anticausal**
	GIES	unknown	**anticausal**	**anticausal**	**anticausal**	**anticausal**	**anticausal**	**anticausal**	**anticausal**	**anticausal**	**anticausal**
	PC	unknown	**anticausal**	**anticausal**	**anticausal**	**anticausal**	**anticausal**	**anticausal**	**anticausal**	**anticausal**	**anticausal**
	ICD	**anticausal**	**anticausal**	**anticausal**	**anticausal**	**anticausal**	**anticausal**	**anticausal**	**anticausal**	**anticausal**	**anticausal**
	RAI	unknown	unknown	unknown	unknown	unknown	unknown	unknown	unknown	unknown	unknown
	FCI	**anticausal**	**anticausal**	**anticausal**	**anticausal**	**anticausal**	**anticausal**	**anticausal**	**anticausal**	**anticausal**	**anticausal**
	LINGAM	unknown	unknown	unknown	unknown	unknown	unknown	unknown	unknown	unknown	unknown
	CCDR	causal	causal	**anticausal**	**anticausal**	**anticausal**	**anticausal**	**anticausal**	**anticausal**	**anticausal**	**anticausal**
	Our method	p=0.0000 **anticausal**	p=0.0000 **anticausal**	p=0.0000 **anticausal**	p=0.0000 **anticausal**	p=0.0000 **anticausal**	p=0.0000 **anticausal**	p=0.0000 **anticausal**	p=0.0000 **anticausal**	p=0.0000 **anticausal**	p=0.0000 **anticausal**
Usps (anticausal)	GES	**anticausal**	**anticausal**	causal	**anticausal**	causal	**anticausal**	causal	causal	**anticausal**	causal
	GIES	**anticausal**	**anticausal**	causal	**anticausal**	causal	**anticausal**	causal	causal	**anticausal**	causal
	PC	causal	unknown	unknown	unknown	causal	**anticausal**	unknown	causal	**anticausal**	unknown
	ICD	unknown	unknown	unknown	unknown	unknown	unknown	unknown	unknown	unknown	unknown
	RAI	unknown	unknown	unknown	unknown	unknown	unknown	unknown	unknown	unknown	unknown
	FCI	**anticausal**	**anticausal**	**anticausal**	unknown	**anticausal**	**anticausal**	**anticausal**	**anticausal**	**anticausal**	**anticausal**
	LINGAM	**anticausal**	**anticausal**	**anticausal**	**anticausal**	**anticausal**	**anticausal**	**anticausal**	**anticausal**	**anticausal**	**anticausal**
	CCDR	causal	causal	causal	causal	causal	causal	causal	causal	causal	causal
	Our method	p=0.0000 **anticausal**	p=0.0000 **anticausal**	p=0.0000 **anticausal**	p=0.0000 **anticausal**	p=0.0000 **anticausal**	p=0.0000 **anticausal**	p=0.0000 **anticausal**	p=0.0000 **anticausal**	p=0.0000 **anticausal**	p=0.0000 **anticausal**
Waveform (anticausal)	GES	**anticausal**	causal	causal	causal	causal	causal	causal	causal	**anticausal**	causal
	GIES	**anticausal**	causal	causal	causal	causal	causal	causal	causal	**anticausal**	causal
	PC	**anticausal**	**anticausal**	**anticausal**	**anticausal**	**anticausal**	**anticausal**	**anticausal**	**anticausal**	**anticausal**	**anticausal**
	ICD	**anticausal**	**anticausal**	**anticausal**	**anticausal**	**anticausal**	**anticausal**	**anticausal**	**anticausal**	**anticausal**	**anticausal**
	RAI	unknown	unknown	unknown	unknown	unknown	unknown	unknown	unknown	unknown	unknown
	FCI	**anticausal**	**anticausal**	**anticausal**	**anticausal**	**anticausal**	**anticausal**	**anticausal**	**anticausal**	**anticausal**	**anticausal**
	LINGAM	**anticausal**	**anticausal**	**anticausal**	**anticausal**	**anticausal**	**anticausal**	**anticausal**	**anticausal**	**anticausal**	**anticausal**
	CCDR	causal	causal	causal	causal	causal	**anticausal**	causal	causal	**anticausal**	causal
	Our method	p=0.0000 **anticausal**	p=0.0000 **anticausal**	p=0.0000 **anticausal**	p=0.0000 **anticausal**	p=0.0000 **anticausal**	p=0.0000 **anticausal**	p=0.0000 **anticausal**	p=0.0000 **anticausal**	p=0.0000 **anticausal**	p=0.0000 **anticausal**
Digit1 (anticausal)	GES	**anticausal**	causal	causal	**anticausal**	causal	causal	causal	causal	causal	causal
	GIES	**anticausal**	causal	causal	**anticausal**	causal	causal	causal	causal	causal	causal
	PC	causal	**anticausal**	**anticausal**	causal	**anticausal**	unknown	unknown	**anticausal**	unknown	unknown
	ICD	unknown	unknown	unknown	unknown	unknown	unknown	unknown	unknown	unknown	unknown
	RAI	unknown	unknown	unknown	unknown	unknown	unknown	unknown	unknown	unknown	unknown
	FCI	**anticausal**	**anticausal**	**anticausal**	**anticausal**	**anticausal**	**anticausal**	**anticausal**	**anticausal**	**anticausal**	**anticausal**
	LINGAM	**anticausal**	**anticausal**	**anticausal**	**anticausal**	**anticausal**	**anticausal**	**anticausal**	**anticausal**	**anticausal**	**anticausal**
	CCDR	**anticausal**	**anticausal**	**anticausal**	**anticausal**	**anticausal**	**anticausal**	**anticausal**	**anticausal**	**anticausal**	**anticausal**
	Our method	p=0.0000 **anticausal**	p=0.0000 **anticausal**	p=0.0000 **anticausal**	p=0.0000 **anticausal**	p=0.0000 **anticausal**	p=0.0000 **anticausal**	p=0.0000 **anticausal**	p=0.0000 **anticausal**	p=0.0000 **anticausal**	p=0.0000 **anticausal**
Pair0047 (anticausal)	GES	anticausal	anticausal	anticausal	anticausal	unknown	unknown	unknown	unknown	unknown	unknown
	GIES	anticausal	anticausal	anticausal	anticausal	unknown	unknown	unknown	unknown	unknown	unknown
	ICD	anticausal	anticausal	anticausal	anticausal	unknown	unknown	unknown	unknown	unknown	unknown
	RAI	unknown	unknown	unknown	unknown	unknown	unknown	unknown	unknown	unknown	unknown
	LINGAM	unknown	unknown	unknown	unknown	unknown	unknown	unknown	unknown	unknown	unknown
	CCDR	causal	causal	causal	causal	causal	causal	causal	causal	causal	causal
	Our method	p=0.0000 **anticausal**	p=0.0000 **anticausal**	p=0.0000 **anticausal**	p=0.0000 **anticausal**	p=0.0000 **anticausal**	p=0.0000 **anticausal**	p=0.0000 **anticausal**	p=0.0000 **anticausal**	p=0.0000 **anticausal**	p=0.0000 **anticausal**

D.5 Influence of Norm Choice to RoCA

	SynCausal						
	0%	Ins-10%	Ins-20%	Ins-30%	Sym-10%	Sym-20%	Sym-30%
l_0	causal ($p = 0.109$)	causal ($p = 0.100$)	causal ($p = 0.106$)	causal ($p = 0.105$)	causal ($p = 0.688$)	causal ($p = 0.607$)	causal ($p = 0.135$)
l_2	causal ($p = 0.198$)	causal ($p = 0.414$)	causal ($p = 0.136$)	causal ($p = 0.277$)	causal ($p = 0.965$)	causal ($p = 0.874$)	causal ($p = 0.111$)
l_∞	causal ($p = 0.399$)	causal ($p = 0.258$)	causal ($p = 0.154$)	causal ($p = 0.104$)	causal ($p = 0.901$)	causal ($p = 0.946$)	causal ($p = 0.164$)

	SynAnticausal						
	0%	Ins-10%	Ins-20%	Ins-30%	Sym-10%	Sym-20%	Sym-30%
l_0	anticausal ($p = 0.000$)	anticausal ($p = 0.000$)	anticausal ($p = 0.000$)	anticausal ($p = 0.000$)	anticausal ($p = 0.000$)	anticausal ($p = 0.000$)	anticausal ($p = 0.000$)
l_2	anticausal ($p = 0.000$)	anticausal ($p = 0.000$)	anticausal ($p = 0.000$)	anticausal ($p = 0.000$)	anticausal ($p = 0.000$)	anticausal ($p = 0.000$)	anticausal ($p = 0.000$)
l_∞	anticausal ($p = 0.000$)	anticausal ($p = 0.000$)	anticausal ($p = 0.000$)	anticausal ($p = 0.000$)	anticausal ($p = 0.000$)	anticausal ($p = 0.000$)	anticausal ($p = 0.000$)

Table 7: Performance of RoCA when using different norms to generate instance-dependent label noise for our noise injection on synthetic causal and anticausal datasets.

E Pseudocode of Our Instance-Dependent Noise Generation

Algorithm 1 Generation of Instance-dependent Noisy Labels

```
Require: An average noise level $\rho$; A sample $S = \{(X_i, \tilde{Y}_i)\}_{i=0}^m$, where contains $C$ number of classes, and $X \in \mathbb{R}^d$.
Initialize an empty list $A$ with length $m$.
for each $i^{th}$ example $(x_i, \tilde{y}) \in S$: do
    Let $a_i = ||X_i||_1$ and add $a_i$ into $A$.
end for
Sort the values in $A$ in ascending order.
Sample a vector $P \in \mathbb{R}^m$ from a $m$-dimensional truncated normal distribution with mean $\rho$, upper limit 1, and lower limit 0.
Sort the values in $P$ in ascending order.
for $i$ in range $(0, m)$: do
    Let the individual flip rate of the $i^{th}$ example $\rho_{x_i}$= (the $i^{th}$ element in $P$).
end for
Generate the instance-dependent noisy label of the $i^{th}$ example $\tilde{Y}^{\rho_{x_i}}$ using the flip rate $\rho_{x_i}$.
```

F Proofs

In this section, we show all the proofs. We remind some notations first.

- Let $\mathcal{X}$ be the instance space and C the set of all possible classes.
- Let $S = \{(x_i, \tilde{y}_i)\}_{t=0}^m$ be an sample set.
- Let $h : \mathcal{X} \to \{1, \ldots, C\}$, be a hypothesis that predicts pseudo labels of instances. Concretely, it can be a K-means algorithm together with the Hungarian algorithm which matches the cluster ID to the corresponding pseudo labels. Let $\mathcal{H}$ be the hypothesis space, where $h \in \mathcal{H}$.
- Let $\tilde{R}^\rho(h) = \mathbb{E}_{(\boldsymbol{x}, \tilde{y}^\rho) \sim P(\boldsymbol{X}, \tilde{Y}^\rho)}[\mathbb{1}_{\{h(\boldsymbol{x}) \neq \tilde{y}^\rho\}}]$be the expected disagreement $\tilde{R}(h)$ between pseudo labels and generated labels $\tilde{y}^\rho$ with ρ-level noise injection.
- Let $\hat{\tilde{R}}_S^\rho(h)$ be the average disagreement (or empirical risk) of h on the set S after ρ-level noise injection.

Firstly, we illustrate the Rademacher complexity bound.

Definition 3 (The Rademacher Complexity Bound (Mohri et al., 2018))**.** Let $\mathcal{H}$ be a family of functions taking values in $\{-1, +1\}$, and let $\mathcal{D}$ be the distribution over the input space $\mathcal{X}$. Then, for any $\delta > 0$, with probability at least $1 - \delta/2$ over a sample $S = (x_1, \ldots, x_m)$ of size m drawn according to $\mathcal{D}$, for any function $h \in \mathcal{H}$,

$$\hat{R}_S(h) - R(h) \leq 2\hat{\mathfrak{R}}_S(\mathcal{H}) + 3\sqrt{\frac{\log\frac{4}{\delta}}{2n}}, \tag{6}$$

where $R(h)$ is the expected risk of the function h, and $\hat{R}_S(h)$ is the empirical risk of the function h on the sample S (Mohri et al., 2018). Specifically, let c be a target concept, then,

$$R(h) = \mathbb{E}_{x\sim\mathcal{D}}[\mathbb{1}_{\{h(x_i)\neq c(x_i)\}}],\ \hat{R}_S(h) = \frac{1}{m}\sum_{i=1}^{m}\mathbb{1}_{\{h(x_i)\neq c(x_i)\}}.$$

F.1 Proof of Theorem 1

Proof. Under causal setting, h random guess the clean labels, i.e., $\forall i, j \in C \wedge i \neq j \wedge \forall t \in \{0, 1, \ldots, m\}$, $P(Y' = y'|Y = y, X = x) = \frac{1}{C}$. Then we will prove that if h can only random guess the clean labels, then h can only random guess the observed labels that contain the label error, i.e., $\tilde{R}(h, x) = \frac{C-1}{C}$.

By the assumption that for every instance and clean class pair (x, y), its observed label $\tilde{y}$ is obtained by a noise rate ρ_x such that $P(\tilde{Y} = \tilde{y}|Y = y, \boldsymbol{X} = x) = \frac{\rho_x}{C-1}$ for all $\tilde{y} \neq y \wedge \tilde{y} \in C$, the risk $\tilde{R}(h, x)$ of h on x and its observed labels comes from two parts:

- When h misclassifies the clean label, h also misclassifies the observed label, i.e., ($y \neq y'$ and $y' \neq \tilde{y}$).
- When h successfully classifies the clean label, h misclassifies the observed label, i.e., ($y = y'$ and $y' \neq \tilde{y}$).

Specifically, the expected risk of each example is as follows.

$$\begin{aligned}
\tilde{R}(h, x) &= R(h, x)(1 - \frac{\rho_x}{C-1}) + (1 - R(h, x))\rho_x \\
&= \frac{C-1}{C}\frac{C-1-\rho_x}{C-1} + \frac{\rho_x}{C} \\
&= \frac{C-1-\rho_x}{C} + \frac{\rho_x}{C} \\
&= \frac{C-1}{C}.
\end{aligned} \tag{7}$$

Because our noise is designed to also satisfy the assumption, after injecting our designed instance-dependent noise, the risk $\hat{\tilde{R}}_S^{\rho^1}(h)$ and $\hat{\tilde{R}}_S^{\rho^2}(h)$ under two different (expected) noise levels $\rho^1 = \mathbb{E}_x[\rho_x^1]$ and $\rho^2 = \mathbb{E}_x[\rho_x^2]$ does not change under the anticausal setting.

$$\tilde{R}^{\rho^1}(h, x) = \tilde{R}(h, x)(1 - \frac{\rho_x^1}{C-1}) + (1 - \tilde{R}(h, x))\rho_x^1 = \frac{C-1}{C}. \tag{8}$$

$$\tilde{R}^{\rho^2}(h, x) = \tilde{R}(h, x)(1 - \frac{\rho_x^2}{C-1}) + (1 - \tilde{R}(h, x))\rho_x^2 = \frac{C-1}{C}. \tag{9}$$

The above equations show that after injecting two different levels of instance-dependent label noise, the risks do not change. For completeness, we also illustrate the convergence rate of the difference between two empirical risks with respect to sample size. By employing the Rademacher complexity bound, with a probability $1 - \delta/2$,

$$\begin{aligned}
&\hat{\tilde{R}}_S^{\rho^1}(h) \leq \mathbb{E}_x[\tilde{R}^{\rho^1}(h,x)] + 2\hat{\mathfrak{R}}_S(\mathcal{H}) + 3\sqrt{\frac{\log\frac{4}{\delta}}{2m}} \\
=&\tilde{R}^{\rho^1}(h) + 2\hat{\mathfrak{R}}_S(\mathcal{H}) + 3\sqrt{\frac{\log\frac{4}{\delta}}{2m}},
\end{aligned}$$

similarly,

$$\begin{aligned}
&\hat{\tilde{R}}_S^{\rho^2}(h) \leq \mathbb{E}_x[\tilde{R}^{\rho^2}(h,x)] + 2\hat{\mathfrak{R}}_S(\mathcal{H}) + 3\sqrt{\frac{\log\frac{4}{\delta}}{2m}} \\
=&\tilde{R}(h,\rho^2) + 2\hat{\mathfrak{R}}_S(\mathcal{H}) + 3\sqrt{\frac{\log\frac{4}{\delta}}{2m}}.
\end{aligned}$$

By applying the symmetric property of the Rademacher complexity bound to the above two inequalities, with a probability $1 - 2\delta$,

$$\begin{aligned}
&|\hat{\tilde{R}}_S^{\rho^1}(h) - \tilde{R}^{\rho^1}(h)| \leq 2\hat{\mathfrak{R}}_S(\mathcal{H}) + 3\sqrt{\frac{\log\frac{4}{\delta}}{2m}} \text{ and} \\
&|\hat{\tilde{R}}_S^{\rho^2}(h) - \tilde{R}(h,\rho^2)| \leq 2\hat{\mathfrak{R}}_S(\mathcal{H}) + 3\sqrt{\frac{\log\frac{4}{\delta}}{2m}}.
\end{aligned}$$

Combining the above two inequalities, we get

$$|\hat{\tilde{R}}_S^{\rho^1}(h) - \tilde{R}^{\rho^1}(h) - \hat{\tilde{R}}_S^{\rho^2}(h) + \tilde{R}(h,\rho^2)| \leq 4\hat{\mathfrak{R}}_S(\mathcal{H}) + 6\sqrt{\frac{\log\frac{4}{\delta}}{2m}}.$$

By Eq. 8 and Eq. 9, the expected risk $\tilde{R}^{\rho^1}(h) = \mathbb{E}_X\left[\tilde{R}^{\rho^1}(h,x)\right] = \mathbb{E}_X\left[\frac{C-1}{C}\right]$ and $\tilde{R}(h,\rho^2) = \mathbb{E}_X\left[\tilde{R}^{\rho^2}(h,x)\right] = \mathbb{E}_X\left[\frac{C-1}{C}\right]$ both equals to $\frac{C-1}{C}$, then the above inequality becomes

$$|\hat{\tilde{R}}_S^{\rho^1}(h) - \hat{\tilde{R}}_S^{\rho^2}(h)| \leq 4\hat{\mathfrak{R}}_S(\mathcal{H}) + 6\sqrt{\frac{\log\frac{4}{\delta}}{2m}}, \tag{10}$$

with a probability 1-2δ, which completes the proof. □

F.2 Proof of Theorem 2

Proof. The expected risk on the observed label for each instance x is that:

$$\begin{aligned}
\tilde{R}^{\rho}(h,x) &= \tilde{R}(h,x)(\frac{\rho_x}{C-1}) + (1 - \tilde{R}(h,x))(1-\rho_x) \\
&= \rho_x + \tilde{R}(h,x) - \rho_x\tilde{R}(h,x) - \frac{\rho_x\tilde{R}(h,x)}{C-1}.
\end{aligned}$$

Then the expected risk of the distribution of observed data is that:

$$
\begin{aligned}
\tilde{R}^{\rho}(h) &= \mathbb{E}_X\left[\tilde{R}^{\rho}(h,x)\right] \\
&= \mathbb{E}_X\left[\rho_x + \tilde{R}(h,x) - \rho_x\tilde{R}(h,x) - \frac{\rho_x\tilde{R}(h,x)}{C-1}\right] \\
&= \mathbb{E}_X\left[\tilde{R}(h,x)\right] + \mathbb{E}_X\left[\rho_x - \rho_x\tilde{R}(h,x) - \frac{\rho_x\tilde{R}(h,x)}{C-1}\right] \\
&= \tilde{R}(h) + \mathbb{E}_X\left[\left(1 - \tilde{R}(h,x) - \frac{\tilde{R}(h,x)}{C-1}\right)\rho_x\right] \\
&= \tilde{R}(h) + \mathbb{E}_X\left[\left(1 - \frac{C\tilde{R}(h,x)}{C-1}\right)\rho_x\right]. \qquad (11)
\end{aligned}
$$

Moving $\tilde{R}(h)$ to the LHS of the above equation completes the proof. □

Note that the convergence rate of $\mathbb{E}\left[\left(1 - \frac{C\tilde{R}(h,x)}{C-1}\right)\rho_x\right]$ can also be directly derived by replacing the expected risks with the empirical risks in Eq. 11. This process employs Inequality 6 and shares a similar conceptual foundation as the proof for the coverage rate presented in Theorem 1.

G Discussion on Assumptions

Firstly, our method is based on some common assumptions in causal discovery: causal minimality, absence of latent confounders, and independent causal mechanisms (Peters et al., 2014).

To ensure that the disagreements under different noise levels remain constant in a causal setting when employing RoCA, we need an additional assumption to constrain the types of label errors in datasets. Specifically, it assumes that for every instance and clean class pair (x, y), the observed label $\tilde{y}$ is derived with a noise rate ρ_x such that $P(\tilde{Y} = \tilde{y}|Y = y, \boldsymbol{X} = x) = \frac{\rho_x}{C-1}$ for all $\tilde{y} \neq y \wedge \tilde{y} \in C$. Note that most types of label errors defined in previous work satisfy this conditional, including random classification label errors (Wang et al., 2019), asymmetric label errors (Scott et al., 2013), manifold label errors (Cheng et al., 2022), and part-dependent label errors (Xia et al., 2020). Note that, pairflip label errors (Han et al., 2018) do not satisfy this condition. In this case, our method can not be directly applied. To utilize our method, existing techniques for learning with label errors can be applied first to estimate clean labels. Specifically, methods such as those proposed by Liu & Tao (2016) and Patrini et al. (2017) can be used initially. These methods are statistically consistent, ensuring that the clean labels can be uniquely identifiable under pairflip label noise. Once we have the estimated clean labels, our method can then be applied to instances $\boldsymbol{X}$ and their estimated clean labels to determine the causal direction.

Additionally, the choice of a backbone clustering method can influence the effectiveness of our approach. Specifically, when dealing with an anticausal dataset, our method relies on a clustering algorithm capable of extracting useful information from $P(\boldsymbol{X})$ to predict $P(Y|\boldsymbol{X})$, rather than making completely random guesses. Thanks to the recent successes of unsupervised and self-supervised methods, some techniques based on contrastive learning (Niu et al., 2021) have achieved competitive performance, with over 90% accuracy, compared to supervised methods on benchmark image datasets such as *CIFAR10* and *MNIST*. We also anticipate that more advanced unsupervised methods will be developed in the future, further enhancing the utility of our approach.